

Mechanical Feedback from Active Galactic Nuclei in Galaxies, Groups, and Clusters

B. R. McNamara^{1,2,3,4} & P. E. J. Nulsen^{3,5}

ABSTRACT

The radiative cooling timescales at the centers of hot atmospheres surrounding elliptical galaxies, groups, and clusters are much shorter than their ages. Therefore, hot atmospheres are expected to cool and to form stars. Cold gas and star formation are observed in central cluster galaxies but at levels below those expected from an unimpeded cooling flow. X-ray observations have shown that wholesale cooling is being offset by mechanical heating from radio active galactic nuclei. Feedback is widely considered to be an important and perhaps unavoidable consequence of the evolution of galaxies and supermassive black holes. We show that cooling X-ray atmospheres and the ensuing star formation and nuclear activity are probably coupled to a self-regulated feedback loop. While the energetics are now reasonably well understood, other aspects of feedback are not. We highlight the problems of atmospheric heating and transport processes, accretion, and nuclear activity, and we discuss the potential role of black hole spin. We discuss X-ray imagery showing that the chemical elements produced by central galaxies are being dispersed on large scales by outflows launched from the vicinity of supermassive black holes. Finally, we comment on the growing evidence for mechanical heating of distant cluster atmospheres by radio jets and its potential consequences for the excess entropy in hot halos and a possible decline in the number of distant cooling flows.

Subject headings: galaxies clusters: general — intergalactic medium — X-rays: galaxies: clusters

¹Department of Physics & Astronomy, University of Waterloo, Waterloo, ON, Canada

²Perimeter Institute for Theoretical Physics, Waterloo, ON, Canada

³Harvard-Smithsonian Center for Astrophysics, 60 Garden St, Cambridge, MA 02138

⁴email: mcnamara@uwaterloo.ca

⁵email: pnulsen@cfa.harvard.edu

1. Introduction

The large scale structure of the Universe revealed by WMAP (Spergel et al. 2007; Komatsu et al. 2011), distant supernovae (Perlmutter et al. 1999; Riess et al. 2000), and galaxy clusters (Vikhlinin et al. 2009; Mantz et al. 2010; Allen et al. 2011) agrees remarkably well with the Λ CDM cosmogony (Davis et al. 1985). However, additional physics is needed to explain the numbers and distribution of baryons in galaxies and galaxy clusters. Gas dynamical models of dark matter halos incorporating radiative cooling and gravitational heating alone produce too much cold gas, too many young stars, and too few hot baryons (Balogh et al. 2001; Davé et al. 2001; Bregman 2007). The level of overcooling leads to model galaxy luminosities, colors, disk and bulge sizes, and so forth that fail to match observations. A similar problem is found on larger scales. Hydrodynamic models have difficulty reproducing the central gas densities, temperatures, entropy distributions, and baryon fractions of the hot atmospheres of clusters (for excellent reviews, see Voit 2005; Borgani & Kravtsov 2009).

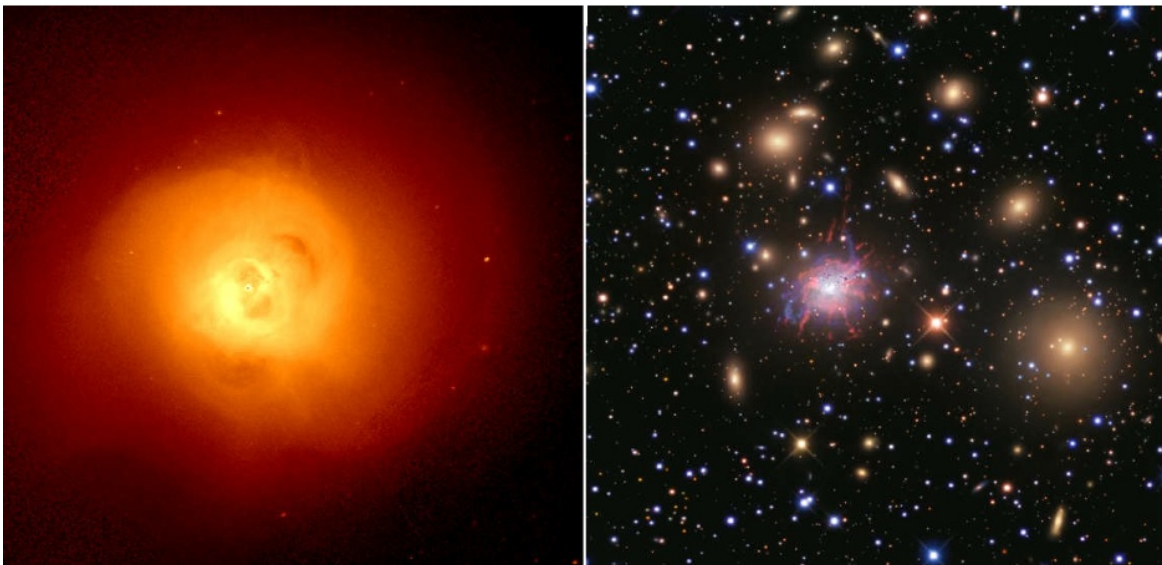


Fig. 1.— *Left:* Deep *Chandra* X-ray image of the Perseus cluster (Fabian et al. 2011). *Right:* Matched optical image of Perseus cluster showing the extensive system of line-emitting filaments around NGC 1275 (Fabian et al. 2011). The images are 11.8 arcmin from N to S.

The formation and evolution of the stars and gas (baryons) are more complicated than the evolution of dark matter halos. Dark matter is governed almost exclusively by gravity. Baryons respond to more complex processes, such as heating, cooling, transport processes, and energetic feedback from supernova explosions and active galactic nuclei (AGN). Evi-

dently, outflows and winds powered by supernovae and by accretion onto supermassive black holes (SMBHs) play a significant role in the evolution of galaxies at essentially all stages of their development (for reviews see Alexander & Hickox 2011; Veilleux et al. 2005). For example, energetic outflows have been detected using emission and absorption line features from distant radio galaxies (e.g., Nesvadba et al. 2006; Morganti et al. 2007; Lehnert et al. 2011), quasars (e.g., de Kool et al. 2001; Chartas et al. 2007; Rupke & Veilleux 2011), and starburst galaxies (Heckman et al. 1990, 2000; Martin 2005; Alexander et al. 2010). Quasar winds capable of sweeping galaxies of their gas may be the primary agent driving the co-evolution of massive galaxies and SMBHs (Silk & Rees 1998; Di Matteo et al. 2005). Star formation in galaxies lying along the so-called main sequence of galaxy formation (Noeske et al. 2007; Tacconi et al. 2010) at redshift $z \sim 2$ and below may be maintained by outflowing gas launched by supernova explosions and inflowing cold accretion flows (Finlator & Davé 2008; Davé et al. 2011b). Supernova and AGN feedback may drive the rapid evolution of galaxies from the blue to the red sequences (Baldry et al. 2004; Schawinski et al. 2007; Hickox et al. 2009). Finally, AGN feedback is probably quenching cooling flows in galaxies and clusters and preventing star formation.

The theory of galaxy formation has advanced significantly with the addition of simple feedback prescriptions into traditional semianalytic and hydrodynamic galaxy formation models (e.g., Kauffmann et al. 1993; Somerville & Primack 1999; Baugh 2006; Springel & Hernquist 2003). Recent studies have shown that a plausible combination of supernova and AGN feedback is able regulate the growth of galaxies by heating or expelling gas from halos (Sijacki & Springel 2006; Bower et al. 2006; Croton et al. 2006; Bower et al. 2008). A triumph was achieved when models incorporating radio (mechanical) AGN feedback occurring at late times reproduced the observed luminosity function of massive galaxies (Bower et al. 2006; Croton et al. 2006; Davé et al. 2011a; Gabor et al. 2011). Modeling the luminosity function of galaxies while simultaneously reproducing the observed properties of the hot atmospheres surrounding them is a further challenge (Bower et al. 2008; McCarthy et al. 2010).

Evidence for a genuine AGN feedback cycle has emerged from X-ray observations of the hot atmospheres of galaxy clusters. A wealth of data collected by the *XMM-Newton* and *Chandra* X-ray observatories has shown that radio AGN are probably the principal agent heating the hot atmospheres of galaxies, clusters, and groups and suppressing cooling flows. The process works roughly as follows: The atmosphere cools and condenses into molecular clouds that form stars and feed the supermassive black hole concealed within the BCG. Nuclear accretion and black hole spin produce mechanically-powerful radio AGN that heat the cooling atmosphere, slowing the rate of cooling, and the cycle repeats. Star formation is suppressed almost entirely in elliptical galaxies, keeping them “red and dead.”

Here we discuss the primary observational evidence for this cycle, concentrating on the spectacular X-ray images of cavities, shock fronts, and filaments embedded in hot atmospheres (Figs. 1 and 2). We briefly discuss observations at longer wavelengths that track the cooling gas and star formation through the final phase of the feedback cycle. We comment on some of the theoretical problems challenging a more complete understanding, including how the central engine is powered, how jet power is coupled to the surrounding hot atmospheres, and recent advances in plasma physics. We discuss new evidence for metal-enriched outflows, and the growing literature dealing with AGN feedback in distant clusters.

This Focus Issue brings together articles dealing with the physics of galaxy clusters, several of which are closely related to ours. In keeping with the spirit of this volume, we make no attempt to present a comprehensive review of what in recent years has grown to a vast literature. Instead we focus on several topics of interest to us and refer the reader to other contributions to this volume and to several comprehensive reviews on related topics: cooling flows (Fabian 1994), elliptical galaxies (Mathews & Brighenti 2003), X-ray clusters and cosmology (Voit 2005; Allen et al. 2011), X-ray spectroscopy of clusters (Peterson & Fabian 2006), feedback in X-ray clusters, groups, and galaxies (McNamara & Nulsen 2007; Blanton et al. 2010; Gitti et al. 2011a), extragalactic radio jets (Worrall 2009), feedback in galaxies (Cattaneo et al. 2009), and the outstanding and comprehensive review of the history of black holes and AGN in the Universe by Alexander & Hickox (2011).

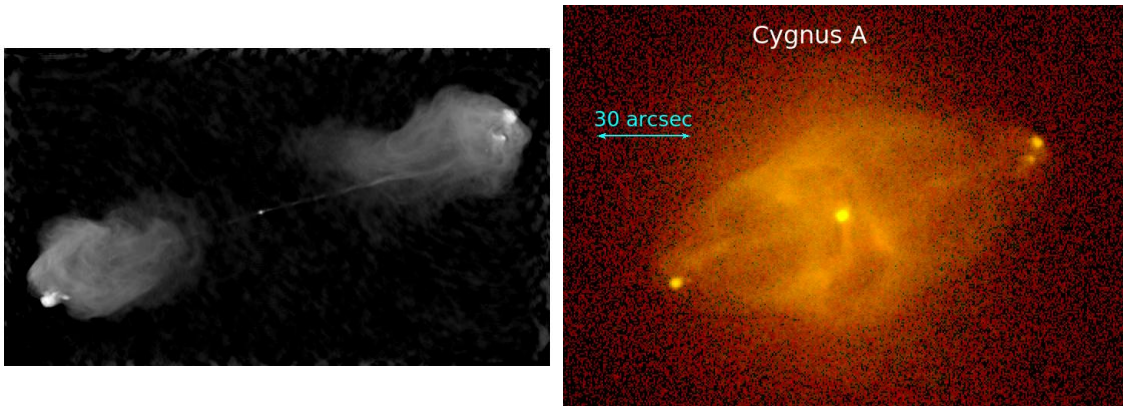


Fig. 2.— *Left:* Cygnus A, 6 cm VLA radio image (Perley et al. 1984). *Right:* *Chandra* X-ray image of Cygnus A. The AGN and radio hotspots are visible in both images. Complex structure, including cavities and the cocoon shock can be seen in the X-ray image (Smith et al. 2002).

2. X-ray Cavities as Gauges of Jet Power

The radiative cooling time at the centers of hot atmospheres in groups and clusters is often less than 1 Gyr. In elliptical galaxies it lies below 0.1 Gyr. Unless the thermal energy being radiated away is replenished, the gas will cool and accrete onto the central galaxy and form stars (Fabian 1994). The end products of cooling in the forms of cold molecular clouds and star formation are observed in many BCGs (Johnstone et al. 1987; Edge 2001; Salomé & Combes 2003; O’Dea et al. 2008), but at levels far below those expected from persistent cooling over the ages of clusters. Other potential repositories include nearly invisible low-mass stars (Fabian et al. 1982; Sarazin & O’Connell 1983; Jura 1986) or neutral hydrogen clouds spread throughout clusters (Haynes et al. 1978). The failure to find a long-term repository in cold gas and stars led many to conclude that very little gas is actually cooling to low temperatures. Several mechanisms that would heat the gas and prevent it from cooling have been suggested over the years, including dynamical friction (Miller 1986a), thermal conduction from the hot outer atmospheres of clusters (Rosner & Tucker 1989; Bregman & David 1988), and AGN (Pedlar et al. 1990; Tucker & David 1997; Soker et al. 2001; Binney & Tabor 1995). However, atmospheric heating models have only recently gained traction.

X-ray images of the Perseus and Cygnus A clusters taken with the *ROSAT* observatory were the first to show radio AGN interacting strongly with the hot atmospheres surrounding them (Boehringer et al. 1993; Carilli et al. 1994). Cavities and filamentary structure in the atmospheres of both clusters are located near the central radio sources. Discoveries of structure in the atmospheres of other clusters soon followed (Sarazin et al. 1995; Rizza et al. 2000). With its leap in spatial and spectral resolution, the *Chandra* X-ray observatory revealed cavities, shock fronts, and cool filaments near the central radio sources in essentially all cooling flow clusters it has observed. Noting the close association between the radio lobes and X-ray cavities in Hydra A, McNamara et al. (2000) pointed out that cavity volumes multiplied by their surrounding pressures provide a gauge of the pV work (mechanical energy) expended as the cavities are inflated. Assuming the cavity dynamics are governed by buoyancy, their ages and in turn mean jet power, were estimated (McNamara et al. 2000; Churazov et al. 2002; Birzan et al. 2004). *Chandra* has since provided what are arguably the most reliable measurements of jet power in dozens of galaxies and clusters. These measurements have led to the understanding that cooling atmospheres in clusters and giant elliptical galaxies are regulated by AGN feedback.

The total enthalpy, i.e., the pV work plus the internal energy that provides the pressure supporting the cavities, is given by

$$H = \frac{\gamma}{\gamma - 1} pV = \begin{cases} 2.5pV, & \text{for } \gamma = 5/3 \\ 4pV, & \text{for } \gamma = 4/3 \end{cases}, \quad (1)$$

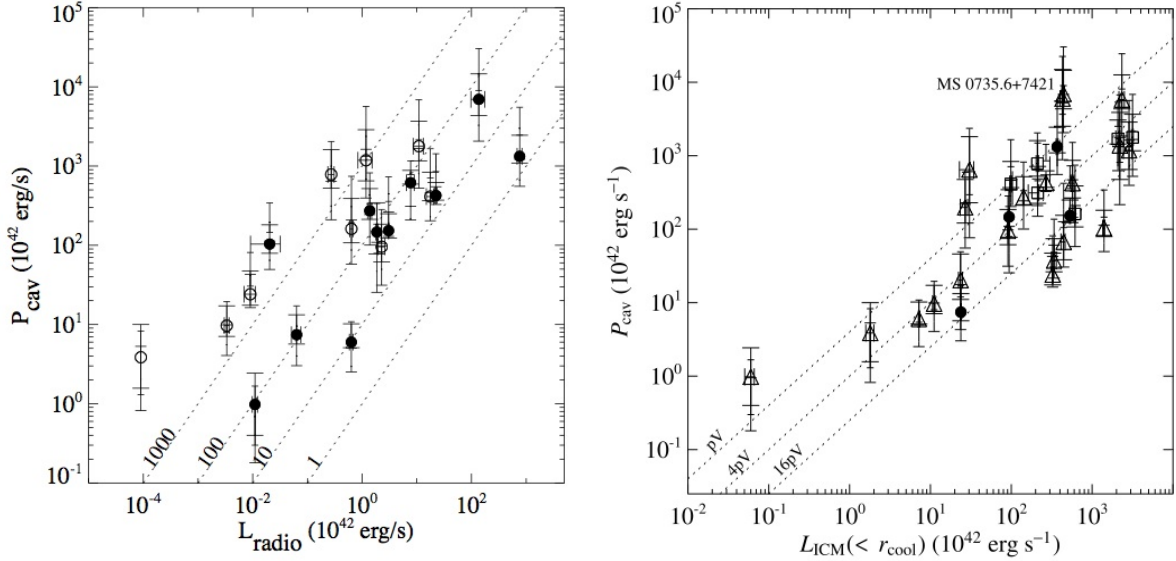


Fig. 3.— *Left*: Cavity power vs. broadband radio power for a sample of cool core clusters (Bîrzan et al. 2008). *Right*: Cavity power vs. X-ray power radiated from the region where the cooling time is shorter than 7.7 Gyr (Rafferty et al. 2006).

where γ is the ratio of specific heats of the cavity plasma. The appropriate ratio of specific heats depends on whether the pressure support within cavities is supplied primarily by relativistic plasma ($\gamma = 4/3$) or nonrelativistic plasma ($\gamma = 5/3$). Were the radio lobes filled with a dilute thermal plasma in local pressure equilibrium, its temperature must exceed roughly 20 keV in order to avoid detection by its thermal X-ray emission (Blanton et al. 2003; Gitti et al. 2007). Such a plasma would presumably have been heated by shocks or cosmic rays stemming from the AGN outburst. More likely, the cavities are filled with relativistic plasma from the radio jets yielding $H = 4pV$ per cavity. Of course, cavities may be filled with more complex gas mixtures. Ideally, the prefactor multiplying pV would take full account of the work done by an expanding cavity (the energy radiated is generally negligible). Using the enthalpy allows $1pV$ for the work. But since the pressure confining an expanding cavity probably decreases as it expands, this is generally an underestimate. The work done depends on how quickly the cavities were inflated and, more generally, the history of each AGN outburst. Observations select for large, mature, cavities such that the canonical $4pV$ per cavity is roughly consistent with MHD simulations (Mendygral et al. 2011). The $4pV$ approximation may be less accurate for cavities inflated by cosmic rays (Mathews & Brighenti 2008). ALMA observations of the Sunyaev-Zeldovich effect, which is most sensitive to nonrelativistic electrons (Pfrommer et al. 2005) will help to determine the composition of the lobe plasma.

The synchrotron power of radio jets and lobes represents a minor fraction of their total power (e.g., Scheuer 1974). It should be no surprise that radio AGN, which are observed in most BCGs centered in cooling flows, were long ago suspected to play a significant role in quenching cooling flows (e.g., Burns 1990; Pedlar et al. 1990; Baum & O’Dea 1991; Tabor & Binney 1993; Tucker & David 1997). However, radio-based estimates of their mechanical power relied critically on the unknown ratio, k , of the energy in non-radiating particles to that in the synchrotron emitting electrons, assumed to lie in the range 0 – 100 (see Willott et al. 1999). A low value of k would provide too little mechanical energy to offset cooling; higher values were possible but received little observational support.

As a consequence of high atmospheric pressures, $\sim 10^{-10}$ dyne cm $^{-2}$, and large cavity diameters, typically 20 kpc but upward of 200 kpc in cases, *Chandra* revealed that relatively modest radio sources may carry extraordinarily large mechanical powers. Fig. 3 *left* shows a plot of cavity power against bolometric radio power for a sample of radio AGN in clusters and groups (Bîrzan et al. 2008). The diagonal lines represent fixed ratios between cavity power and synchrotron luminosity. On average, the mean mechanical power is 100 times larger than the synchrotron power, and in some instances ~ 1000 times larger. With mechanical jet power exceeding 10^{45} erg s $^{-1}$, many radio sources rival the radiative output of a quasar. Their mechanical power is comparable to or exceeds the X-ray luminosities of their cooling atmospheres. The high mechanical (jet) powers relative to their synchrotron luminosities implies that hydrodynamical radio sources are governed on large scales by heavy particles, i.e., $k \gg 10$ (Dunn & Fabian 2006; Bîrzan et al. 2008; De Young 2006; Hardcastle & Croston 2010). If jets are launched as light particles or Poynting flux (Diehl et al. 2008; De Young 2006; Nakamura et al. 2008), their radio lobes, which fill the cavities, must be energetically dominated by heavy particles that were presumably entrained from the surrounding atmosphere (Croston 2008).

3. Quenching Cooling Flows

A significant consequence of high jet powers is their ability to offset radiative cooling of the atmospheres surrounding them (Bîrzan et al. 2004; Rafferty et al. 2006; Dunn & Fabian 2006; Best et al. 2006; Dong et al. 2010). Fig. 3 *right* shows average cavity power plotted against the X-ray cooling luminosity for a sample of clusters. Lines of equality between cooling and heating are shown for injected energies of $1pV$, $4pV$, and $16pV$ per cavity. The diagram shows that $\simeq 4pV$ per cavity is typically observed, which is enough to offset cooling in most systems (McNamara & Nulsen 2007). AGN power output is variable. Objects move up or down in P_{cav} depending on when they are observed. Therefore, the current power, low

or high with respect to the $4pV$ line, may not equal its long term average.

Selection effects are at issue in Fig. 3. At high cooling luminosities, the cavity detection fraction is about 70% (Dunn & Fabian 2006). With the general bias against detection (McNamara & Nulsen 2007), their result implies that nearly all strong cooling flows harbor powerful cavity systems. At the same time, we are aware of no powerful systems in low cooling luminosity clusters lying to the left of the pV line. They would be easily detected. We interpret the distribution of points as an envelope sampling the upper end of the distribution of jet powers at a given cooling luminosity, and not a linear correlation. Most importantly, the diagram shows that jet power correlates with the level of cooling: larger cooling flows host increasingly powerful AGN that rival or exceed their cooling luminosities.

Fig. 3 does not include additional power from shocks (David et al. 2001), sound waves (Fabian et al. 2003a; Forman et al. 2005), thermal conduction (Zakamska & Narayan 2003; Voigt & Fabian 2004; Voit 2011), cosmic ray leakage (Mathews & Brighenti 2008), and other forms of energy. On average, cavity enthalpies underestimate the energy deposited in the cooling regions, which only strengthens our view that AGN are energetically able to offset cooling.

Fig. 3 is weighted toward cavity systems in rich clusters. Cavity systems have recently been identified in abundance in the hot atmospheres of groups (Sun et al. 2009; Dong et al. 2010; Gitti et al. 2010; Giacintucci et al. 2011; O’Sullivan et al. 2011a) and ellipticals (Cavagnolo et al. 2010; Nulsen et al. 2009; Mulchaey & Jeltama 2010). These studies have shown that radio AGN in groups and ellipticals are energetically significant with respect to the thermal energy content of their atmospheres (Gaspari et al. 2011a; McCarthy et al. 2010).

The upshot is AGN feedback is operating at the centers of cooling atmospheres spanning seven decades in X-ray luminosity between $\sim 10^{38}$ erg s $^{-1}$ and 10^{45} erg s $^{-1}$. This is significant because other heating processes such as thermal conduction and dynamical friction are unimportant in the atmospheres of groups and ellipticals. That AGN feedback is operating over such a broad scale suggests it is the primary mechanism stabilizing cooling flows in galaxies, groups, and rich clusters.

3.1. Scatter in Cavity Power vs Cooling Luminosity Diagram

The scatter in Fig. 3 *right* is largely real. We find no correlation between this scatter and physical parameters, including central gas and stellar densities, host galaxy luminosity, synchrotron age, and so forth. As deeper *Chandra* images yielding better cavity measurements have become available, it is becoming clear to us that measurement uncertainty contributes

to the scatter beyond the errors shown in Fig. 3. The error bars reflect the uncertainties in the spheroidal geometry. In many cases, cavity sizes and locations are measured using underexposed *Chandra* images that are unable to reveal the extent of the cavity. In addition, irregular shapes add uncertainty to estimates of their volume and location within a cluster. This in turn adds uncertainty to the estimate of the surrounding pressure. Finally, many cavities are surrounded by thick rims. It is unclear whether the inner, outer, or midpoint of the rim represents the true radius and hence, the displaced volume of the cavity. While this technique is straightforward, unavoidable complications contribute significantly to the uncertainty of the measurements. Deeper images combined with more objective measuring techniques are needed to reduce the measurement error.

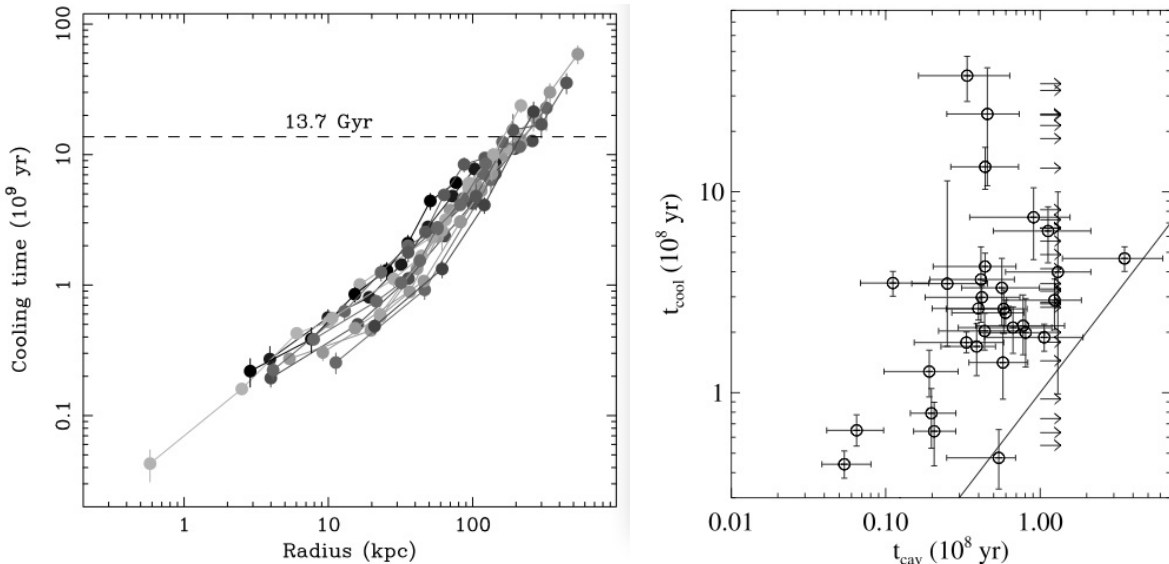


Fig. 4.— *Left*: Cooling time vs. radius for the sample of Voigt & Fabian (2004). *Right*: Cooling time vs. cavity age from (Rafferty et al. 2008).

4. Maintaining X-ray Atmospheres through Mechanical Feedback

The list of processes unrelated to AGN that can heat the hot intracluster gas continues to expand and it is too long to cover in any detail here. The most important distinction among potential heating processes is whether or not they involve feedback. The great majority of proposed heating processes, including thermal conduction (e.g., Narayan & Medvedev 2001), turbulent heat diffusion (e.g., Ruszkowski & Oh 2011), heating associated with mergers (e.g., ZuHone et al. 2010; Birnboim & Dekel 2011) dynamical friction (e.g., Miller 1986b; Kim

et al. 2005) and heating by off center AGN (Hart et al. 2009), involve no evident feedback mechanism, hence no means for heating rates to be tuned to match radiative cooling. For these to account for the observed state of clusters we must appeal to accidental coincidence between average heating and cooling rates.

4.1. Heating vs. cooling

The terms “heating” and “cooling” still cause confusion when applied to cool core clusters. Radiative losses from gas in a fixed volume would reduce its temperature. However, in an atmosphere confined by gravity, the heat loss due to radiation is counteracted by adiabatic compression under the weight of overlying gas, so that the sign of the net temperature change is indeterminate. Under realistic conditions, heat loss can result in a temperature rise. Conversely, heat input to a gravitationally confined atmosphere does not necessarily increase the gas temperature. Apart from any heat exchange, other forms of energy input (e.g., the increase in potential energy when gas is pushed outward by inflating lobes) complicate this issue further. Thus, “heating” is frequently associated with a decrease in gas temperature, while “cooling” can cause the temperature to increase.

While the indeterminate temperature change creates ambiguity, the sense of heat transfer does not. Here, “cooling” always refers to heat loss (by radiation) from the gas. Its invariable physical consequence is a reduction in the specific entropy of the gas, regardless of the change in temperature. Similarly, “heating” always refers to the addition of heat to the gas, which invariably causes an increase in its specific entropy (Voit & Donahue 2005).

4.2. Demands of the High Incidence of Short Cooling Times

In terms of the specific entropy, S , the energy equation of the gas is

$$\rho T \frac{dS}{dt} = \mathcal{H} - \mathcal{R}, \quad (2)$$

where ρ is the gas density, T is its temperature, \mathcal{H} is the heating rate per unit volume and \mathcal{R} is the power radiated per unit volume. This may be expressed as

$$\frac{d}{dt} \ln K = \frac{1}{t_h} - \frac{1}{t_c}, \quad (3)$$

where $K = kT/n_e^{\gamma-1}$ is the entropy index and n_e is the electron density. The cooling time is the time required for the gas to radiate its thermal energy,

$$t_c = \frac{p}{(\gamma - 1)\mathcal{R}}, \quad (4)$$

and the analogous heating time is

$$t_h = \frac{p}{(\gamma - 1)\mathcal{H}}. \quad (5)$$

For most heating mechanisms, the effect of excess cooling is to increase the dominance of cooling over heating and *vice versa*, destabilizing the balance between heating and cooling. If cooling dominates, it tends to run away, so that the gas will cool to low temperatures. When heating dominates, the gas is driven toward a state where (equation 3) $t_h \simeq t$, the age of the system, in which case the cooling time would be $t_c = t_h \mathcal{H} / \mathcal{R} \gg t$. Thus, we should expect to see long cooling times in systems where heating dominates.

In the absence of feedback, typical heating rates must be sufficient to offset radiative cooling. Otherwise cooled gas would be deposited at rates of many hundreds of solar masses per year in many clusters, in conflict with observations (Peterson et al. 2003; Peterson & Fabian 2006). On the other hand, if the balance is tipped in favor of heating, we should expect typical cooling times in excess of the Hubble time. This is in conflict with the observed high fraction of short cooling times. For example, 44% of the HIFLUGCS sample have central cooling times shorter than 1 Gy (Hudson et al. 2010). This issue is even sharper for lower mass systems. Their lower temperatures suppress thermal conduction, and there is less dynamical activity to drive heating. At the same time, their central cooling times are often shorter than those in rich clusters (Sun et al. 2009, and this volume).

Thus, while heating that does not involve feedback can certainly reduce the demands on the process that prevents copious amounts of gas from cooling to low temperatures in clusters, a process involving feedback is required to account for the high incidence of short cooling times. The prime candidate is AGN heating.

4.3. Observational Evidence for a Feedback Loop

A true AGN feedback loop, as opposed to simple AGN heating, must couple the AGN energy output to the reservoir of gas fueling it. Apparently, this applies to the hot atmospheres of galaxies, groups, and clusters. The trend in Fig. 3 *right* shows not only that radio AGN are powerful enough to offset cooling, but that atmospheres with larger X-ray cooling luminosities host more powerful AGN. In other words, the X-ray luminosity of the cooling gas measured on tens of kiloparsec scales, and the jet power maintained by accretion of gas near the AGN on subparsec scales, are apparently in causal contact. We do not understand how energy emitted from such a small volume couples itself so efficiently to gas on such vastly larger scales.

The prevalence of short central cooling times is another indication that hot atmospheres are maintained by feedback. Despite the high energetic output of AGN, the radiative cooling time of the gas surrounding them remains well below one Gyr. Fig. 4 *left* (Voigt & Fabian 2004) shows cooling time profiles for the hot atmospheres of several cooling clusters. The cooling time profiles steadily decline from about 14 Gyr at a radius of 200 kpc to a few 10^8 yr within the BCG. They are typical of atmospheres experiencing powerful AGN activity. Instead of shutting down cooling entirely, cooling flows are stable and long lived.

We shall illustrate this point using an extreme example. At 10^{62} erg, MS0735.6+7421 (MS0735) is experiencing what is arguably the most energetic AGN heating event known (McNamara et al. 2005). Yet its central cooling time is only 5×10^8 yr, which is only a few times longer than the age of the outburst. Assuming its AGN quenched cooling entirely and the cooling flow shut down today, cooling would reestablish itself and AGN activity would resume in only several hundred Myr. The most powerful AGN in clusters do not dramatically raise the temperature or lower the density of the gas in their vicinity. Instead, they raise the central entropy of the gas through a surprisingly gentle “heating” process that restores potential energy to the atmosphere that was lost by radiation (Voit & Donahue 2005; Cavagnolo et al. 2009; Pratt et al. 2010; Gaspari et al. 2011b). This entropy boost is shown as a flattening of the central atmospheric entropy profiles compared to a pure cooling atmosphere (Voit & Donahue 2005) and in the correlation between jet power and the value of the central entropy of the host’s hot atmosphere (Pfrommer et al. 2011), which are both shown here in Fig. 5. The southwest shock of Centaurus A, which boosts the local gas temperature by an order of magnitude, is a counter example (Croston et al. 2009). However, such strong temperature boosts are not seen in rich clusters.

Finally, AGN are generally active on timescales comparable to or shorter than the central cooling timescales, a condition that is needed to prevent rapid cooling and puddling of cold gas in BCGs. Fig. 4 *right* shows central cooling time plotted against cavity buoyancy timescales with which we estimate the age of the AGN outbursts. The plot shows that cavities are usually younger than the time it takes for the gas they are rising through to cool. In other words, AGN activity recurs frequently enough to prevent runaway cooling.

4.4. Metal-Enriched Outflows

Hot atmospheres surrounding clusters and galaxies are chemically enriched by stellar evolution processes taking place in galaxies over time (Arnaud et al. 1992; Borgani et al. 2008; Fabjan et al. 2010). The gas is chemically enriched to average level of approximately 1/3 of the solar value. However, the metallicity approaches and can exceed the solar value in

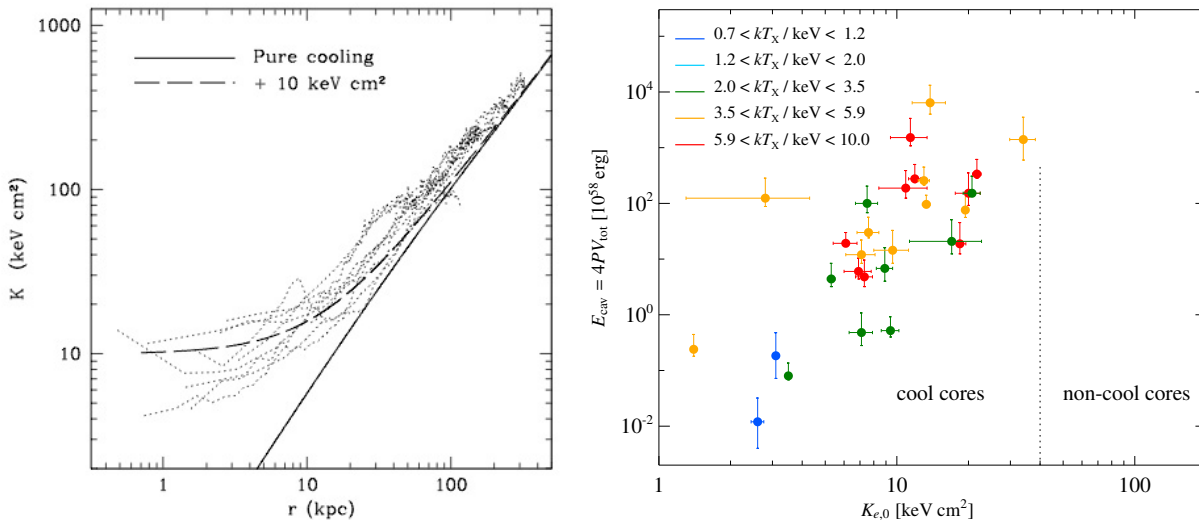


Fig. 5.— Left panel shows atmospheric entropy profiles for a sample of cooling flow (cool core) clusters from Voit & Donahue (2005). The central entropy values lie above the pure cooling model. The right panel shows central entropy values plotted against jet (cavity) power (Pfrommer et al. 2011). The correlation shows that AGN are raising the central entropy. Marker colors are indicated in the figure.

the vicinity of the BCG (Allen & Fabian 1998; Dupke & White 2000; De Grandi & Molendi 2001; De Grandi et al. 2004; de Plaa et al. 2007). This is shown in Fig. 6 from De Grandi et al. (2004). The metallicity reaches a maximum near the solar value at the location of the BCG. The gas has been enriched primarily by SN Ia ejecta. The central metallicity peak is broader than the stellar light profile indicating that metals are diffusing outward, well beyond the stars that created them (Rebusco et al. 2005). Mixing either by mergers or AGN outflows could produce this broadening (Rebusco et al. 2005; Roediger et al. 2007; Rasia et al. 2008; David & Nulsen 2008; Gaspari et al. 2011b), but AGN outflows have recently received strong observational support. Cool, metal-rich, keV gas has been found along the cavities and radio sources of several clusters and groups (e.g., Simionescu et al. 2008, 2009; Kirkpatrick et al. 2009; Gitti et al. 2011b; O’Sullivan et al. 2011b; Werner et al. 2010). The metallicity is enhanced at levels comparable to those near the BCG, and in excess of the surrounding gas lying at the same projected radius. This metal-enriched gas must have been launched out of the BCG along with the radio jets and is being dispersed into the intracluster medium.

The amount of gas being transported outward is substantial. In Hydra A, several $10^7 M_{\odot}$ of iron alone has been lifted more than 120 kpc into the intracluster medium (Simionescu

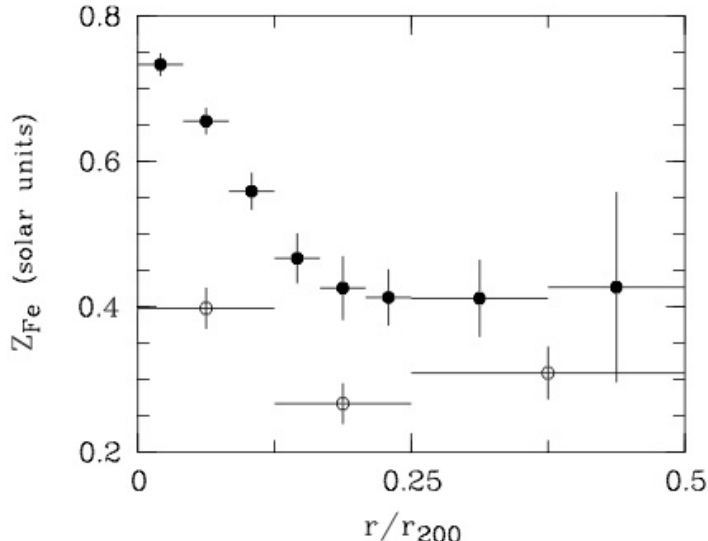


Fig. 6.— Average iron abundance profile from De Grandi et al. (2004). Solid points (open points) represent clusters with (without) a BCG.

et al. 2009; Kirkpatrick et al. 2009). The largest known outflow in the MS0735 cluster can be traced out to an “iron radius” of $R_{\text{Fe}} \simeq 300$ kpc (Fig. 7). Excess metallicity along the jet axis has been found in at least 17 clusters with cavity systems (Kirkpatrick & McNamara in preparation). The iron radius scales surprisingly well with mechanical jet power with the form $R_{\text{Fe}}(\text{kpc}) = 60P_{\text{jet}}^{0.43}$, where jet power is expressed in units of 10^{44} erg s^{-1} (Kirkpatrick et al. 2011, ; Kirkpatrick et al. 2012, in preparation). This scaling is consistent with typical radio AGN displacing metals from the BCG well into the hot halos of clusters, as observed by De Grandi and others (Fig. 6). Kirkpatrick’s scaling relation provides an estimate of the average jet power over several hundred Myr that is independent of more complicated cavity and shock front measurements.

Iron alone represents roughly one part in one thousand of the total mass flowing out with the jets and cavities. In Hydra A, the total outflowing gas mass exceeds $10^{10} M_{\odot}$. This implies an average outflow rate of $\sim 100 M_{\odot} \text{ yr}^{-1}$ over the few 10^8 yr duration of the current outburst. An outflow of this magnitude would reduce the rate of mass deposition and star formation from the cooling flow (McCarthy et al. 2008). A substantial fraction of the energy required to lift the gas is likely to be dissipated when low entropy gas falls back inwards, which could be a significant heat source in the ICM (Gitti et al. 2011b). A flow of this size may be expected to deplete the high metallicity gas at the center (eg., Guo & Mathews 2010). However, after accounting for replenishment of metals from ongoing stellar evolution, AGN

apparently do not erase the central iron peaks entirely, as indicated by recent simulations of gentle feedback (Gaspari et al. 2011b). In fact, they probably prevent excessive central metal enrichment and subsequent overcooling.

A radio AGN’s ability to lift volume-filling gas depends on its mechanical power and not its luminosity. The iron radius is thus limited by the accretion rate onto the black hole in Eddington units. As the SMBH grows and the accretion rate falls below a few percent of the Eddington rate, the AGN is expected to transition from a quasar to a mechanically-dominated radio jet (see Narayan & McClintock 2008 for a review, and below). The transition from a quasar to a radio galaxy would be accompanied by a dramatic rise in the work done by the jet on the volume-filling gas, and a hot outflow would ensue. Thus, the dispersal of metals throughout cluster atmospheres by AGN probably occurred primarily during the later stages of cluster development following the putative quasar phase of the BCG.

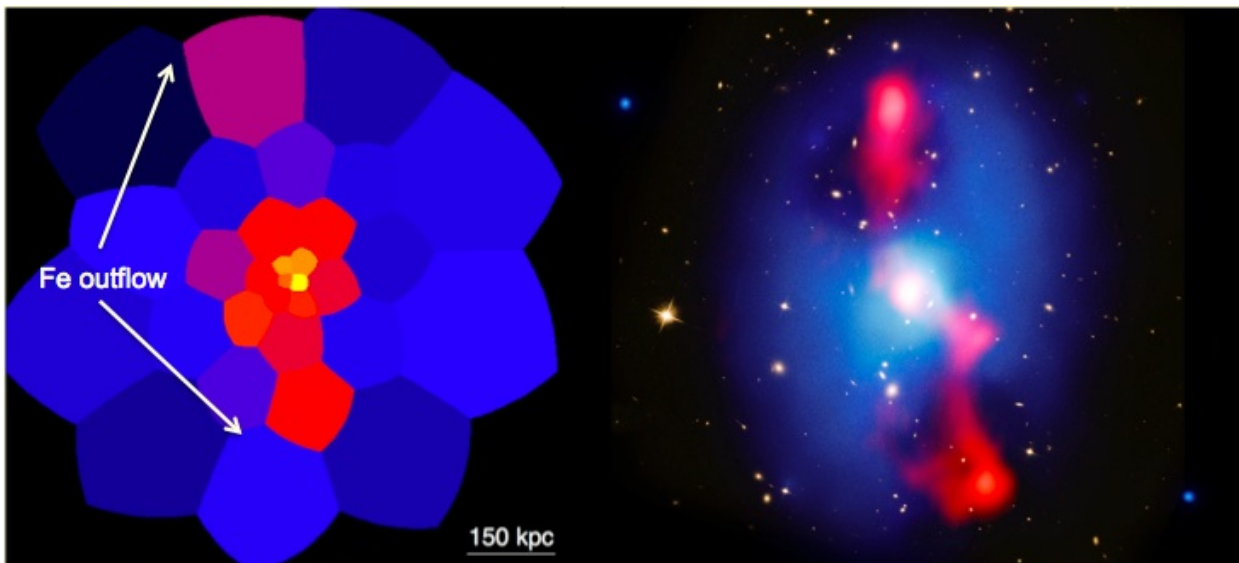


Fig. 7.— *Left*: Abundance distribution in MS0735. Red and purple cells indicate enhanced metal abundance compared to the ambient gas. *Right*: X-ray (blue), radio (red) and optical images of MS0735 on the same scale as the abundance distribution in the left panel.

5. How AGN Outbursts Heat Hot Atmospheres

It remains unclear which processes are communicating the energy of AGN outbursts to the hot atmospheres that host them, or how outburst energy is dissipated in the gas. Even if power flows exclusively via jets into the radio lobes, there are several channels for transferring

the power to the ICM. In the basic model outlined by Scheuer (1974), jets inflate radio lobes which do work on the gas as they expand. Thus, jet power is divided between the lobes and the ICM. A rapidly inflating lobe can drive shocks into the gas, producing edges in X-ray surface brightness that have been observed in a number of objects (e.g., Smith et al. 2002; Jones et al. 2002; Kraft et al. 2003; McNamara et al. 2005; Machacek et al. 2006). However, the typical division between internal energy in the lobes and mechanical work done on the ICM has yet to be assessed (estimates exist for some cases, e.g., Nulsen et al. 2005; Forman et al. 2005; Randall et al. 2011). This energy division also evolves with time.

While theory suggests that the lobes should be unstable to rapid disruption, observations indicate that they can survive for long periods of time (e.g., Fabian et al. 2011). Disruption can be delayed if the instability is suppressed by viscosity (Reynolds et al. 2005), turbulent diffusion (Scannapieco & Brüggen 2008), magnetic stresses (Ruszkowski et al. 2007; O’Neill et al. 2009), or favorable dynamics (Pizzolato & Soker 2006). Regardless of the details, ultimately the lobe plasma is likely to mix with the ICM, depositing cosmic rays and magnetic energy there. In hydrodynamic jet simulations (e.g., Brüggen & Kaiser 2002; Heinz et al. 2006; De Young 2010) heat is transferred to the ICM when lobe gas is mixed with it, but this may be unrealistic. Energy exchange could be much slower if the primary forms of lobe energy that are mixed with the ICM are cosmic rays and magnetic fields (e.g., Boehringer & Morfill 1988; Mathews & Guo 2010).

Cosmic rays should also diffuse out of radio lobes into the surrounding ICM (Boehringer & Morfill 1988; Sijacki et al. 2008). In addition to slow collisional heating, streaming cosmic rays can excite plasma waves that are likely to end up dissipating and acting as another source of heat (Enßlin et al. 2011). Indeed, Guo & Oh (2008) argue that cosmic ray heating powered by the central AGN, coupled with a significant level of thermal conduction can stabilize the cooling gas. If lobes remain intact as they rise buoyantly, they will maintain approximate pressure balance with their surroundings. Their pressure decreases with time causing a decrease in enthalpy that releases energy into the ICM, mostly as kinetic energy in the flow around rising “bubbles” (McNamara & Nulsen 2007).

The larger scale gas flow created by an expanding lobe can be made turbulent by interaction with small cavities left by earlier generations of AGN (Heinz & Churazov 2005), or by interaction with dense clouds (e.g., Edge & Frayer 2003; Salomé & Combes 2003; Salomé et al. 2011). Uplift of low entropy gas with rising cavities and the fallback that is likely to follow (Churazov et al. 2001; Gitti et al. 2011b) and flow around buoyant bubbles can also generate turbulence in the ICM (Sanders et al. 2011). This turbulence will be dissipated, providing yet another channel for dispersing outburst energy into hot atmospheres (e.g., Dennis & Chandran 2005).

While it seems likely that enough energy is being deposited by AGN outbursts to prevent hot atmospheres from cooling to low temperatures, two key issues remain to be resolved: whether enough of the outburst energy is dissipated to prevent the gas from cooling and how that energy is distributed throughout the gas. In the remainder of this section we consider some aspects of heating and cooling in more detail.

5.1. Adiabatic Uplift

The decrease in specific entropy caused by radiative losses is balanced most effectively by dissipative processes that add heat and increase entropy. Beyond energy deposition, dissipation is needed to counteract the heat loss due to radiative cooling. To emphasize this point, we consider what would happen if there was no significant heating in an AGN outburst.

The state of a simple gas is completely determined by its entropy and pressure, so that we only need to consider the effect of the change in gas pressure. Expressed in terms of the cooling function, $\Lambda(T)$, the cooling time (equation 4) is

$$t_c = \frac{p}{(\gamma - 1)n_e n_H \Lambda(T)}, \quad (6)$$

where n_e and n_H are the electron density, and proton density of the gas, respectively. For isentropic gas, $T \propto p^{(\gamma-1)/\gamma}$ and $n_e \propto p^{1/\gamma}$, indicating the pressure dependence of the cooling time. Fig. 8 shows how the cooling time varies under an adiabatic pressure change for gas with solar and half solar abundances. Adiabatic uplift would decrease the pressure. The increase in cooling time as gas is decompressed by 2.5 orders of magnitude, from an initial temperature of $kT = 5$ keV (hotter than the central gas in most cool cores with short central cooling times) is just over a factor of 2 for solar abundances (typical of the central gas in these systems). For half solar abundances the increase is a little over a factor of 3. For observed abundances, in the temperature range of interest, the cooling time is quite insensitive to the pressure. Thus, lifting gas from the center of the cool core to regions of much lower pressure delays cooling to low temperatures by no more than a factor of $\simeq 3$ and, typically, considerably less. For gas with cooling times < 1 Gyr, adiabatic uplift is ineffective as a way to prevent most of the gas from cooling to low temperatures.

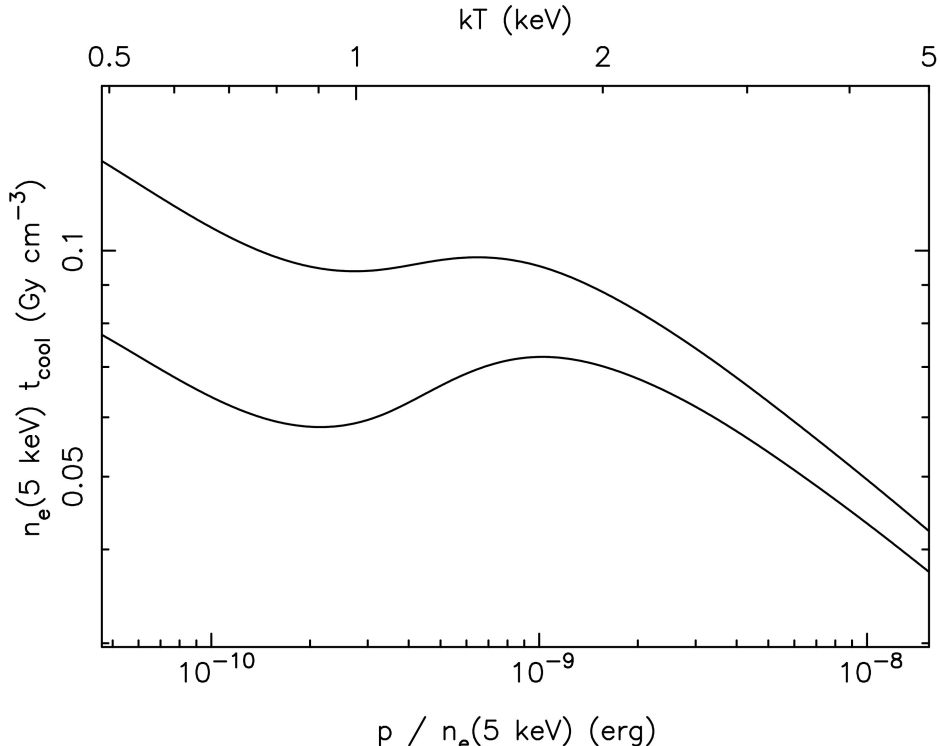


Fig. 8.— Cooling time vs. pressure under adiabatic expansion. Cooling time (Gyr) multiplied by the electron density (cm^{-3}) at 5 keV is plotted against the pressure divided by the electron density at 5 keV for gas with solar (lower curve) and half solar abundances (upper curve), under an isentropic pressure change. The upper scale shows the temperature in keV. The cooling function used is from the APEC model (Smith et al. 2001). Below ~ 2 keV, the increase in the cooling function due to line cooling shortens cooling times significantly. Particularly for $kT \lesssim 3$ keV, typical of the temperature in cool cores, the cooling time is quite insensitive to adiabatic pressure changes.

5.2. Lobe Size and the Spectrum of AGN Outbursts

The timing and power of AGN outbursts, i.e., their power spectra (cf. Nipoti & Binney 2005) are important issues affecting the properties of radio lobes and their effect on the ICM. When an outburst deposits energy, E_{tot} , into a volume, V , the pressure increase is $\sim (\gamma - 1)E_{\text{tot}}/V$. This makes the fractional pressure increase large if the total thermal energy within V , i.e., $\int_V p/(\gamma - 1) dV$, is smaller than E_{tot} . With a large fractional pressure increase, the gas in V would expand rapidly, driving shocks into the surrounding gas. Thus, the smallest volume that can be affected by an AGN outburst contains a thermal energy comparable to the energy deposited by the outburst, placing a lower limit on the sizes of radio lobes and cavities. Conversely, a new outburst injecting energy into an existing radio

lobe can have very little effect on the surrounding gas unless the total energy injected is comparable to its existing internal energy. Sizes and shapes of lobes are also affected by the detailed properties of jets and their interaction with the environment. Lobe size clearly affects where the outburst energy is deposited in the environs of an AGN. That is, the spatial distribution of the outburst energy is an important property for the feedback process.

The average power is another important factor. Even if the jet power is constant, pV generally increases faster than linearly with the radius, making the speed at which a lobe advances decrease with time in the absence of other effects. When the expansion is subsonic, buoyant lift may detach a lobe from its jet and turbulent motions in the surrounding ICM may toss the lobe around. Simulations have shown that turbulence in the ICM driven by the continuing infall of subhalos can have a marked effect on the structure of radio lobes (Brüggen et al. 2005; Heinz et al. 2006). Based on a small set of simulations, Morsony et al. (2010) found that the size of the region affected by an outburst, its “radius of influence,” R , is determined by outburst power, P_j , with $R \propto P_j^{1/3}$. In these simulations, ICM “weather” (turbulence) also leads to relatively isotropic deposition of the AGN energy. While disruption and diffusion is the likely fate of all lobes, a number of systems, such as MS0735.6+7421 (McNamara et al. 2005) and NGC 5813 (Randall et al. 2011), show considerable large-scale symmetry that has survived through multiple outburst cycles.

Other significant properties affected by outburst history are the shapes and relative positions of the cocoon shocks and lobes. While a steady, continuous jet produces highly elongated shock fronts (Vernaleo & Reynolds 2007), simulations (O’Neill & Jones 2010) show that intermittent outbursts can make the fronts and lobes considerably more spherical, as observed. This is illustrated in Fig. 9, which shows synthetic X-ray images from MHD simulations of a pair of jets with a 50% duty cycle at the center of a realistic cluster, from Mendygral, Jones, & Dolag (2012, submitted).

5.3. Weak Shock and Sound Heating

Outburst energy can appear in the gas as thermal, kinetic, or potential energy. Much of its impact is transient. For example, a passing weak shock compresses and heats the gas, accelerating it to a moderate fraction of the sound speed. However, when the shock has passed the gas returns to rest, its pressure settles to slightly less than the preshock pressure because the gas has moved outward where gravity is weaker. A weak shock raises the entropy only slightly, so the reduction in pressure leaves the gas cooler than before the shock passed. Most of the residual energy gain from the shock remains as gravitational potential energy. All this happens in a time that is small compared to the cooling time, so that the transient

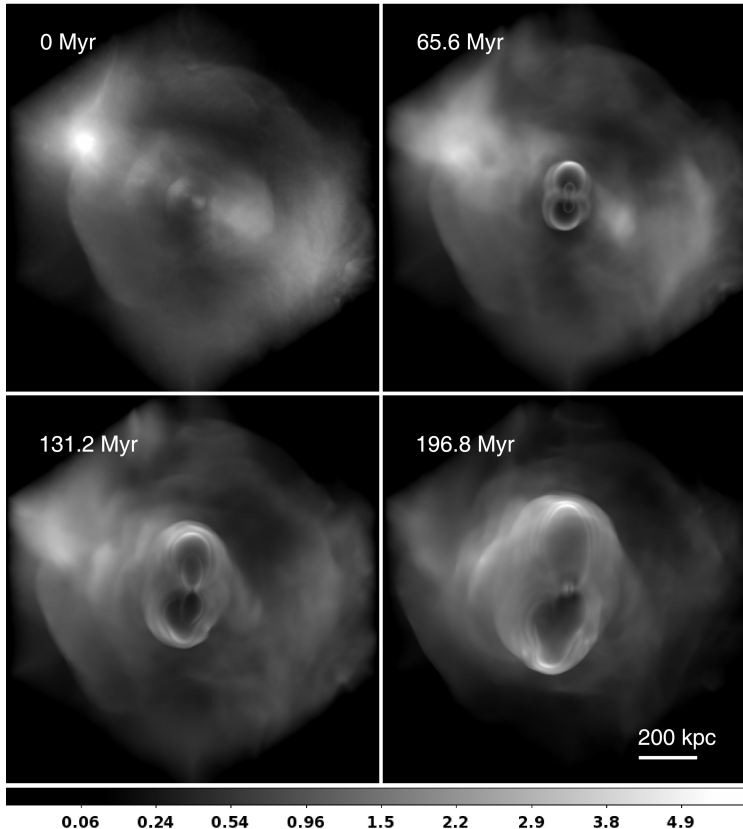


Fig. 9.— Shocks and cavities for a simulated intermittent AGN at a cluster center. These are synthetic broadband X-ray images, divided by a beta model, at various times, made from the MHD simulations of Mendygral et al. (2012). Their simulations represent a pair of intermittent, opposed AGN jets, with 50% duty cycle, at the center of a $\simeq 1.6$ keV cluster extracted from a cosmological simulation. In contrast to the highly elongated lobes and shocks produced by jets with constant power, these lobes and cavities resemble the moderately elliptical systems found in reality.

effects of a single weak shock are largely negligible. Using the example of the Hydra A cluster, David et al. (2001) and Nulsen et al. (2007) argued that weak shock heating fails to compensate for radiative losses in cool cores.

The primary effect of radiation is entropy reduction. The entropy increase in a single weak shock, ΔS , provides an effective heat input of $\Delta Q \simeq T\Delta S = E\Delta \ln K$, where K is the entropy index (see below equation 3), E is the specific energy and $\Delta \ln K$ is the change of $\ln K$ in the shock. The fractional heat input, $\Delta Q/E$, in a single weak shock is small, but the cumulative effect of multiple shocks can be significant. Two nearby, well-observed systems, M87 (Forman et al. 2007) and NGC 5813 (Randall et al. 2011), have experienced multiple

shocks. The time interval between them is short compared to the cooling time. If repeated weak shocking is sustained over long periods of time, it can comfortably compensate for the heat radiated in the inner regions of both M87 and NGC 5813. Because shock strength generally decreases with radius and the entropy increase is cubic in the shock strength, weak shock heating is most effective at small radii. Thus, it appears likely that the process responsible for preventing gas from cooling to low temperatures close to the Bondi radius is weak shock heating in at least these two systems. Given the importance of gas properties at the Bondi radius to feeding of the AGN (see section 7.1), this gives weak shock heating a potentially critical role in the feedback process. Other heating processes are required and are more effective on larger scales.

Sound waves in the Perseus cluster ICM created by repeated outbursts from NGC 1275 could be a significant heat source (Fabian et al. 2003a, 2005a). Thermal conduction and viscosity cause the sound to dissipate, generating significant heat if the transport coefficients are close to their magnetic field free values. Ruszkowski et al. (2004) showed that heating by sound dissipation might also be able to offset cooling in the long term. Whereas weak shock heating depends on the cube of the shock strength (pressure amplitude), sound heating is proportional to the square of the wave amplitude, making it more effective on larger scales. Unfortunately, while the shock heating rate is largely independent of the uncertain transport coefficients, sound heating does depend on them (section 5.5).

5.4. Isotropic Jet Heating

Radio synchrotron jets, such as Cygnus A (Fig. 2), give the impression that the jet’s energy flux is confined to a narrow tube. While this may be true initially as the jets are launched, X-ray and low frequency radio images show that jet power is quickly dissipated over a large solid angle. In canonical systems like M87 (Forman et al. 2007) and Perseus (Fabian et al. 2011), as well as lesser known systems such as NGC 5044 (David et al. 2009) and 2A0335+096 (Sanders et al. 2009), energy is being deposited by multiple cavities, weak shocks, and sound waves that are dissipating energy over much of the volume of the inner atmosphere (Fig. 10). Observations of the Perseus cluster (Fabian et al. 2003a, 2005a), M87 (Forman et al. 2007), Abell 2052 (Blanton et al. 2011) (Fig. 11), Centaurus (Fabian et al. 2005b; Sanders & Fabian 2008) have shown that their AGN generate sound waves of sufficient intensity to heat the central volume of gas. Furthermore, cavities are emerging in multiple directions from the nuclei of the elliptical galaxy NGC 5044 and the BGG in 2A0335+096 (Fig. 10). This may indicate that jets are launched by a series of randomly-oriented accretion disks (King & Pringle 2007), jet precession (Dunn et al. 2006; Gaspari et al. 2011c) and/or

the larger-scale cavities are being blown around by atmospheric pressure gradients (Brüggen et al. 2005; Heinz et al. 2006; Morsony et al. 2010).

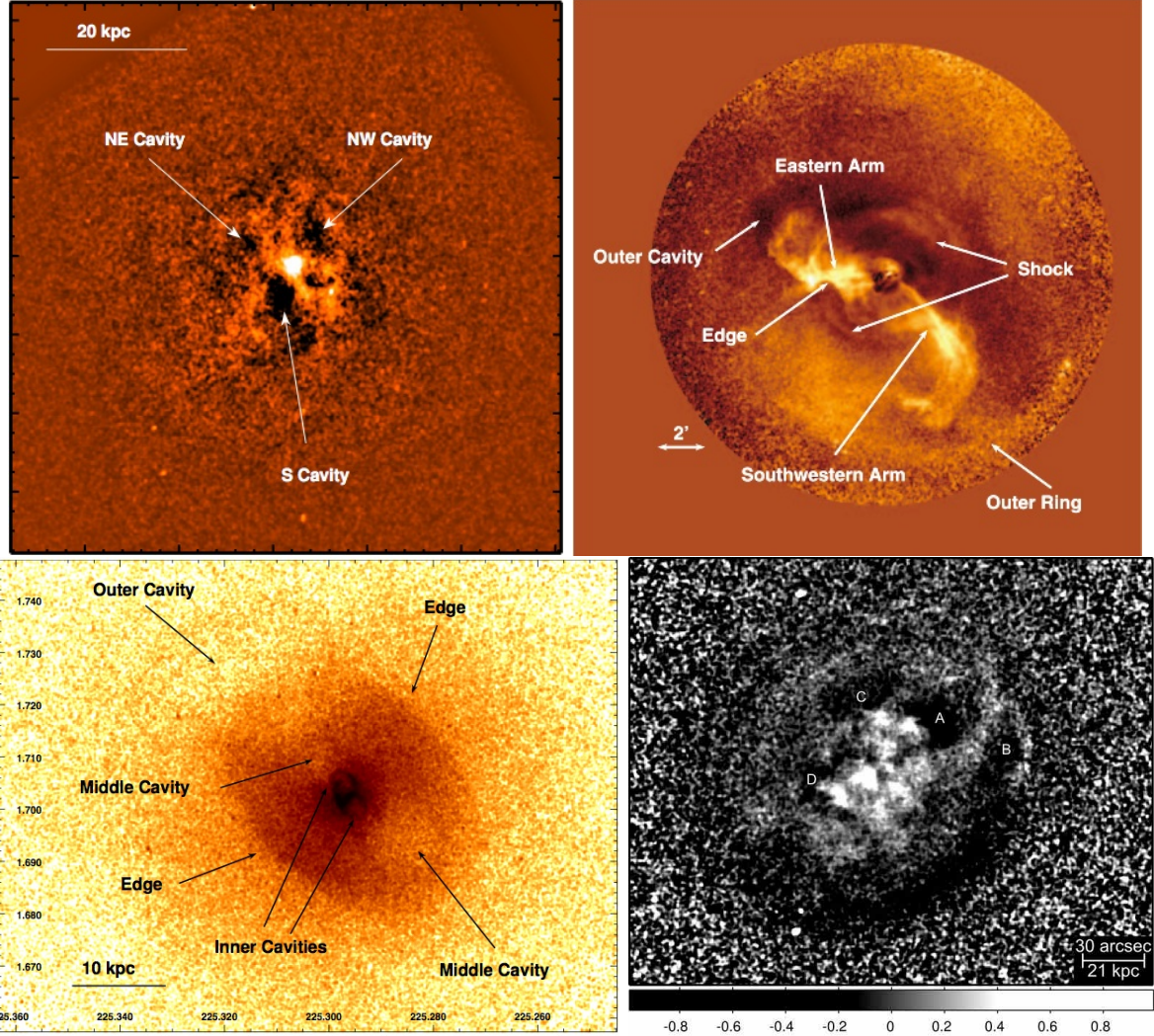


Fig. 10.— Examples of systems showing multiple cavities and shocks. *Upper left*: Unsharp mask 0.3 – 2 keV image of the NGC 5044 group showing multiple cavities (David et al. 2009). *Upper right*: Region around M87 in the Virgo cluster, showing deviations from the azimuthally averaged surface brightness in the energy band 0.5 – 2.5 keV (Forman et al. 2007). *Lower left*: 0.3 – 2 keV image of the NGC 5813 group, showing multiple shock fronts and cavities (Randall et al. 2011). *Lower right*: Unsharp mask image of 2A0335+096 showing multiple cavities and sound waves (Sanders et al. 2009).

Even in cases where jet heating is highly anisotropic, following an outburst the lowest

entropy gas that remains, which is the most in need of heating, falls towards the cluster center. Since the free-fall time is short compared to the cooling time, there is more than enough time for this gas to fall in close to the AGN where it can be heated most effectively in subsequent outbursts. Such circulation is observed in simulations of unidirectional jets (Peter Mendygral, private communication). The need for isotropic heating by apparently anisotropic jets has been cited as a problem by many researchers. In our view, this issue is not as serious as is commonly perceived.

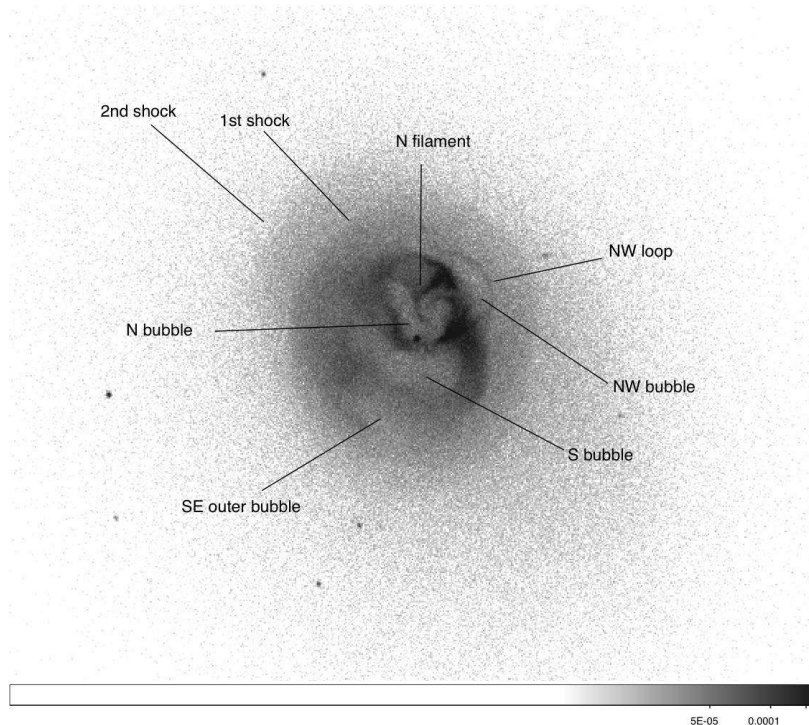


Fig. 11.— Deep, 650 thousand second exposure of Abell 2052 taken with the Chandra X-ray observatory showing multiple cavities and weak shock fronts in the inner 60 kpc of the cluster surrounding the central radio source (Blanton et al. 2011).

5.5. Transport

Poor understanding of the transport properties of hot atmospheres has impeded progress. In the absence of magnetic fields, transport properties are governed by Coulomb collisions. The Coulomb mean free paths for electrons is $\simeq 0.26(kT)^2 n_e^{-1}$ pc and for protons $\simeq 0.37(kT)^2 n_e^{-1}$ pc. Here, kT is given in keV and n_e in cm^{-3} . Thermal conduction would

certainly play a significant role in helping to prevent gas from cooling (e.g., Zakamska & Narayan 2003; Voigt & Fabian 2004) and the viscosity would be dynamically significant (e.g., Fabian et al. 2003b). However, the ratio of the Larmor radius to the mean free path for thermal electrons is $r_{L,e}/\lambda_{ee} \simeq 1.3 \times 10^{-10} n_e (kT)^{-3/2} B_{\mu\text{G}}^{-1}$ and for thermal protons it is $r_{L,p}/\lambda_{pp} \simeq 4 \times 10^{-9} n_e (kT)^{-3/2} B_{\mu\text{G}}^{-1}$, where $B_{\mu\text{G}}$ is the magnetic field strength in μG (typically $B_{\mu\text{G}} \sim \text{few}$ in the ICM, e.g., Carilli & Taylor 2002; Bonafede et al. 2011). The particles are coupled tightly to the magnetic field lines and transport is extremely anisotropic. In the presence of a weak magnetic field tangled by isotropic turbulence, the effective thermal conductivity is expected to be reduced by a factor of $\simeq 3$ (Narayan & Medvedev 2001), presumably with a similar effect on the viscosity. However, the true situation may be far more complex.

5.5.1. *Magnetothermal Instability*

Anisotropic conduction introduces important new effects by making radial temperature gradients unstable. With a negative radial temperature gradient, an atmosphere is subject to the magnetothermal instability (MTI; Balbus 2000; Parrish & Stone 2005). In essence, conduction tends to keep gas on the same field line isothermal. When a parcel of gas lying on a horizontal field line moves outward while maintaining its temperature at the same value as the bulk of the gas on the same field line, it will be hotter than its new surroundings. Then buoyancy makes it rise further, causing instability. Simulations show that MTI drives turbulence and orients the magnetic field preferentially in the radial direction, helping to promote radial heat flux (Parrish et al. 2008).

Negative temperature gradients occur in the outer atmospheres of clusters and throughout non-cool core clusters (e.g., Vikhlinin et al. 2005). However, the temperature gradient is generally positive in cores with short central cooling times, so that MTI is not important for AGN feedback in massive clusters. Less massive hot atmospheres generally have short central cooling times and often do not show temperature drops in the core. These systems may be affected by MTI. However, the steep temperature dependence of the thermal conductivity ($\kappa \sim T^2$, Braginskii 1965) limits the role of conduction at lower temperatures. Since the power available to drive the turbulence cannot exceed the conductive heat flux, MTI will be less vigorous in cooler systems.

5.5.2. Heat Flux Driven Buoyancy Instability

With a positive radial temperature gradient, highly anisotropic conduction makes an atmosphere subject to the heat flux driven buoyancy instability (HBI, Quataert 2008). When the magnetic field is initially parallel to the temperature gradient, there is a steady heat flux, \mathbf{h} , along the field lines. Inclined perturbations then kink the field lines, producing small scale variations in $\nabla \cdot \mathbf{h}$, so that heat is deposited in some regions and removed from others. The resultant heating and cooling can then drive buoyant motions that amplify the perturbations. Like MTI, HBI drives turbulence, but it tends to orient field lines perpendicular to the temperature gradient, strongly suppressing thermal conduction (Bogdanović et al. 2009; Parrish et al. 2009). Under the right circumstances, turbulence driven by HBI and MTI may enhance diffusive transport in the ICM (Sharma et al. 2009).

Cool core clusters generally have positive radial temperature gradients in their cores, and HBI may suppress thermal conduction in them. However, turbulence driven by other processes, including moving subhalos, continuing minor mergers, and AGN activity, can overwhelm the relatively weak effects of HBI, isotropizing the magnetic field and maintaining a relatively high level of thermal conduction. The power available to drive HBI turbulence is also limited by the total conductive heat flux (Parrish et al. 2010). Ruszkowski & Oh (2011) argue further that turbulence driven by moving subhalos in cluster cores is sufficient to make turbulent heat diffusion dominate over conduction there.

5.5.3. Plasma Effects

Typically, the magnetic pressure in the ICM is only a small fraction, $\sim 1\%$, of the gas pressure (Carilli & Taylor 2002; Bonafede et al. 2011), so that the magnetic field is dynamically insignificant. The field has little influence on fluid motions while it is dragged along with it. Thus, gas motions tend to produce changes in the magnetic field strength. In the absence of particle-particle collisions, adiabatic invariance of the magnetic moment would then change the particle velocity dispersion perpendicular to the field, making the pressure anisotropic. Collisions counteract this effect, but the collisional relaxation time for protons in the ICM, $\tau_{pp} \simeq 700(kT)^{3/2}n_e^{-1}$ yr, is long enough that fluid motions can create significant levels of pressure anisotropy.

Schekochihin et al. (2005) argued that when the field is weak, pressure anisotropy due to fluid motions leads to fire hose or mirror instabilities that rapidly strengthen the field until the magnetic pressure is comparable to $\text{Re}^{-1/2}p$, where Re is the Reynolds number. Schekochihin et al. (2010) have identified another plasma instability, gyrothermal instabil-

ity, that is triggered by heat flux along the magnetic field. They argue that gyrothermal instability could limit the parallel heat flux. More generally, they make a strong case that transport properties of the plasma cannot be modeled simply in terms of a conductivity and viscosity like unmagnetized plasmas.

Kunz et al. (2011) argue that these processes can provide a stable local heating mechanism. Assuming that turbulence can maintain the pressure anisotropy close to the margin of the firehose or mirror instabilities, they equate it to the pressure anisotropy resulting from competition between a steadily changing magnetic field and collisional relaxation. This provides a dissipation rate expressed in terms of thermodynamic properties of the fluid and the magnetic field strength that can stably balance radiative cooling. However, this mechanism requires an external source to drive sufficient turbulence to maintain the pressure anisotropy. The primary dissipation channel must also be that associated with the pressure anisotropy, which is generally slow compared to the turnover time of the largest eddies in turbulent systems.

Simulations show that turbulence tends to create an intermittent magnetic field distribution (e.g., Jones et al. 2011). Turbulent motion tends to expel magnetic field from much of the ICM, leaving a weak field occupying most of the volume and strong fields confined to small regions. Little work has been done on the impact of intermittent magnetic field on transport. Nevertheless, the field distribution and the relative sizes of the collisional mean free paths and magnetic field structures are likely to affect transport properties. At present, we can only conclude that transport phenomena in the ICM may be complex. Ignorance may yet prove to be the only basis for assuming that transport in the ICM is any simpler than in the solar wind.

6. The Star Formation-Cooling Time-Entropy Threshold

A link between cooling hot atmospheres and the cold interstellar medium was established thirty years ago with the discovery of bright $H\alpha$ emission in BCGs located in cooling flow clusters (Heckman 1981; Hu et al. 1985; Heckman et al. 1989, e.g., Fig. 1 *right*). Most of these BCGs are forming stars at rates of several to several tens of solar masses per year (Johnstone et al. 1987; McNamara & O’Connell 1989; O’Dea et al. 2008). Their rates dramatically exceed those in normal giant elliptical galaxies and most nearby spirals. Therefore, they cannot be maintained by stellar mass loss. (See Voit & Donahue 2011 for a more nuanced view.) Nevertheless, their star formation rates are only a few percent or less of the rates expected from pure radiative cooling.

The gulf between X-ray cooling rates and star formation rates was for decades the most serious challenge to cooling flow models. This situation changed dramatically when X-ray spectra of cooling flows obtained with the *XMM-Newton* observatory failed to detect emission features from Fe XVII and other species at the expected levels (Peterson et al. 2003; Peterson & Fabian 2006; Sanders et al. 2010). Cooling gas is found with a range of temperatures, but there is less emission from low temperature gas than classical cooling flow models predict (Peterson et al. 2003; Kaastra et al. 2004). Furthermore, the emission measure distribution of the cooling gas is apparently inconsistent with predictions of simple cooling and heating models (Peterson et al. 2003). Despite this problem, once AGN heating is accounted for, the observed star formation rates lie within a factor of a few of the reduced (net) cooling rates (Rafferty et al. 2006; Best et al. 2007; O’Dea et al. 2008; Hudson et al. 2010; Donahue et al. 2010; Hicks et al. 2010). The storied discrepancy between X-ray cooling rates and star formation rates is no longer a serious issue.

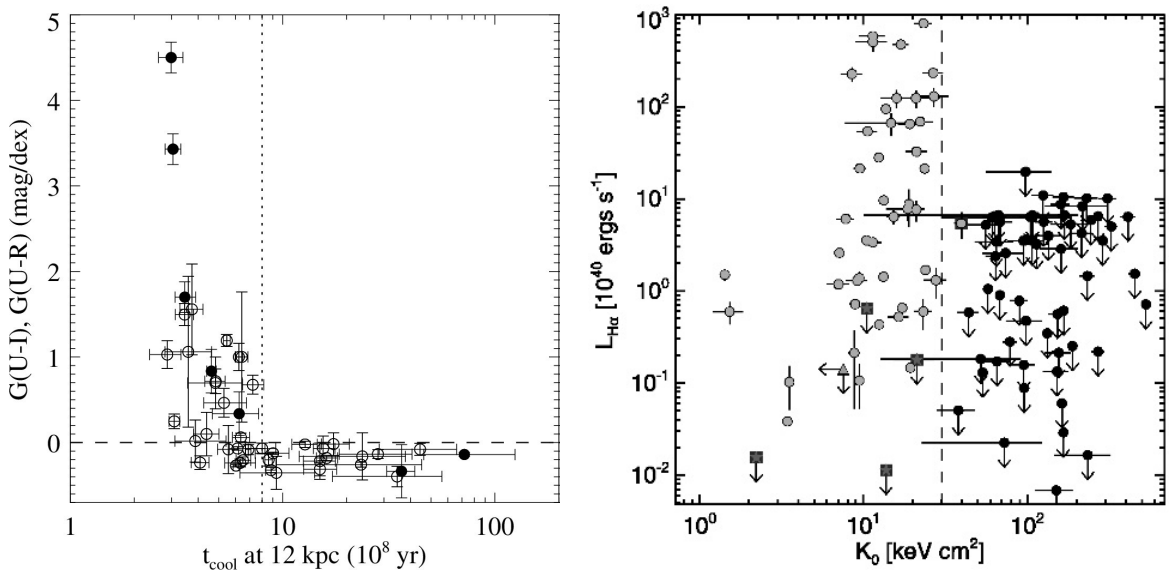


Fig. 12.— *Left*: Color vs. cooling time at 12 kpc (Rafferty et al. 2008). *Right*: $H\alpha$ luminosity vs. central entropy (Cavagnolo et al. 2008). Young stars and line emission nebulae are only seen in BCG’s with short central cooling times, or, equivalently, low central entropies.

The star formation that is observed is almost certainly being fueled by cooling flows. The relationship between short X-ray cooling times and star formation has recently been resolved by *Chandra* into a sharp threshold (Rafferty et al. 2008; Cavagnolo et al. 2008). Central host galaxy color, which is sensitive to star formation, is plotted against the cooling time within the BCG in Fig. 12 *left*. This diagram shows that the colors of BCGs centered in atmospheres with cooling times exceeding $t_{\text{crit}} \sim 5 \times 10^8$ yr are red and thus are not

experiencing significant levels of star formation. However, when the central cooling time falls below t_{crit} , most BCGs become bluer than normal and thus are experiencing substantial levels of star formation. This cooling time threshold corresponds to an entropy threshold of about 30 keV cm^2 , where Cavagnolo et al. (2008) found the onset of $\text{H}\alpha$ emission and radio activity. The tendency for BCGs experiencing star formation to reside in clusters lying above the cluster $L_x - T_x$ relation (Bildfell et al. 2008) is a consequence of the star formation threshold.

The origin of this threshold is unclear. Voit et al. (2008) and Voit (2011) have suggested it appears when gas becomes thermally unstable in the competition between radiative cooling and thermal conduction. Sharma et al. (2011) suggested that for thermal instability to grow and for cooling gas to condense into stars, its growth time must also be shorter than about 10 free-fall times. Other clues to its origin may be gleaned from the red BCGs with short cooling times. These systems are usually offset from the X-ray centroid and may not be accreting gas, or perhaps they are quenched by AGN feedback (Rafferty et al. 2008). Whatever its specific origin may be, the threshold links cooling atmospheres to star formation.

Some have suggested that the cold gas and star formation in BCGs are merger debris or stripped material from donor galaxies (e.g., see Sparks et al. 1989). While this may be true in some cases, it would only account for the prevalence of star formation in cooling cores and the star formation threshold with great difficulty. Galaxies located in the cores of clusters are largely devoid of cold gas and star formation (Best et al. 2007). BCGs in cooling flows are the only nearby population of ellipticals experiencing significant levels of star formation. In the extreme, they harbor $> 10^{10} M_\odot$ of molecular gas (Edge 2001; Salomé & Combes 2003). No known population of galaxies is able to donate molecular gas at this level. The most gas-rich spiral galaxies in nearby clusters contain $\sim 10^9 M_\odot$ or less of molecular gas, and such a galaxy plunging through a cluster would release most of this gas into the ICM before it arrived at the BCG (Kirkpatrick et al. 2011). Gravitational torques may play a role in triggering star formation (Wilman et al. 2009), but galaxy interactions are unable to explain the aggregate star formation and gas properties of BCGs.

7. The Radio AGN Itself

The canonical picture of a radio loud AGN involves a $\sim 10^8 M_\odot$ black hole with a horizon radius of $3 \times 10^{13} \text{ cm}$, a thin accretion disk spanning radii of $\sim 1 - 30 \times 10^{14} \text{ cm}$, and a dusty torus with an inner radius of $\sim 10^{17} \text{ cm}$ (Urry & Padovani 1995). A black hole embedded in 1 keV gas at the cluster center has a Bondi radius of about 10^{19} cm , or a few parsecs. It is usually assumed that AGN are powered by accretion onto the SMBH

(Lynden-Bell 1969; Begelman et al. 1984). But whether energy is released through hot or cold accretion, how power output is related to the structure of the AGN and the spin of the black hole, and how AGN regulate atmospheric cooling on scales of 10^{24} cm are poorly understood. The feedback cycle involves coordinated processes operating over 10 decades in scale, presenting both fundamental and numerical challenges (e.g., Kim et al. 2011) that are currently being dealt with by assumption and approximation.

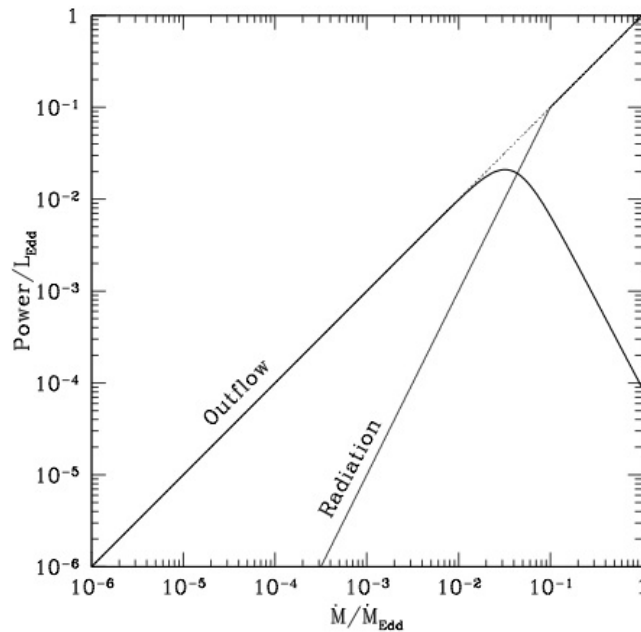


Fig. 13.— Jet power and radiated power in units of the Eddington limit vs. accretion rate in Eddington units (from Churazov et al. 2005). This is a schematic illustration of the transition from low radiative efficiency and high mechanical efficiency at low accretion rates to high radiative efficiency and low mechanical efficiency at high accretion rates.

Unlike radio AGN, quasars and high nebular excitation AGN release energy primarily in the form of radiation generated by dissipation in a thin accretion disk (Shakura & Sunyaev 1973). Radio AGN in clusters and normal ellipticals emit the bulk of their energy not in radiation but in a mechanical form that is accompanied by radio jets and lobes. This form of energy output is thought to be generated by radiatively inefficient accretion from a high pressure, optically thin but geometrically thick, ionized disk (see Narayan & McClintock 2008 for a review). The ions and electrons are out of thermal equilibrium, and their cooling times exceed the flow time onto the SMBH. Therefore, most of the gravitational energy released by the inflow cannot be radiated. The energy is instead carried inward with the accretion flow, although some may be driven outward in a mechanically-dominated jet and/or

a wind, i.e., ADIOS (Blandford & Begelman 1999). Because so little radiation emerges from the accretion flow, they have been dubbed radiatively inefficient accretion flows (RIAF) or advection dominated accretion flows (ADAF).

With the known exceptions of a few distant cooling clusters hosting central quasars (Russell et al. 2010; Crawford et al. 1999b; Siemiginowska et al. 2010), BCGs and ellipticals host RIAFS. Their nuclear X-ray and radio synchrotron luminosities lie below a few percent of their jet powers (Sambruna et al. 2000; Merloni & Heinz 2007; Hlavacek-Larrondo & Fabian 2011; Fabian & Rees 1995). By analogy with black hole binaries (Fender et al. 1999; Merloni et al. 2005; Körding et al. 2008), a quasar or radiation dominated accretion flow forms when the physical accretion rate exceeds a few percent of the Eddington accretion rate (Begelman et al. 1984; Falcke et al. 2004; Merloni et al. 2005; Churazov et al. 2005). The Eddington rate can be expressed as $\dot{M}_{\text{Edd}} = 2.2\epsilon^{-1}M_{\text{BH},9} M_{\odot} \text{ yr}^{-1}$, where ϵ is the conversion efficiency between accretion power and radiated power, which is generally assumed to be ~ 10 percent, and $M_{\text{BH},9}$ is the black hole mass in units of $10^9 M_{\odot}$. For accretion far below the Eddington rate, a high pressure RIAF forms (Narayan & Yi 1994; Blandford & Begelman 1999). As shown here schematically in Fig. 13 (Churazov et al. 2005), AGN power is dominated by mechanical outflows when $\dot{M}/\dot{M}_{\text{Edd}} \ll 1$. When $\dot{M}/\dot{M}_{\text{Edd}}$ exceeds a few percent, the AGN transitions to a quasar and it releases the binding energy of accretion in the form of radiation.

Although the black hole masses in BCGs are all but unknown, their status as the largest galaxies in the Universe ensures that they harbor massive black holes (McConnell et al. 2011). For jet powers $P_{\text{jet}} = 0.1\dot{M}c^2$, accretion rates implied by mechanical jet powers lie in the range $10^{-4} - 10^{-2}$ of the Eddington rate (Rafferty et al. 2006; Hickox et al. 2009; Hlavacek-Larrondo & Fabian 2011), which is well within the RIAF regime. Physical accretion rates typically correspond to several hundredths of a solar mass per year. Only in extreme cases, such as MS0735 and Hydra A, do the implied accretion rates approach or exceed $1 M_{\odot} \text{ yr}^{-1}$. The combination of relatively high jet powers and radiatively inefficient accretion is consistent with nuclear black hole masses exceeding $\sim 10^9 M_{\odot}$. In this picture, quasars at the centers of clusters (e.g., Crawford et al. 1999b) are important because they are accreting at high Eddington rates and may be in transition between radiatively efficient and inefficient AGN (i.e., quasar mode and radio mode).

7.1. Hot Bondi Accretion or Cold Molecular Accretion?

Fueling AGN by spherical Bondi accretion from hot atmospheres is appealing for several reasons. The Bondi mechanism is simple. The accretion rate is related to the temperature and density of the atmosphere at the location of the Bondi radius which is five or six decades

larger than the event horizon. Moreover, Bondi accretion provides a simple feedback mechanism because the Bondi accretion rate for $\gamma = 5/3$ depends on the gas properties only through the entropy index, $K = kT/n_e^{2/3}$, which is the gas property most directly affected by heating and cooling. Most importantly, hot atmospheres are naturally able to provide a steady supply of fuel when the gas is dense enough (i.e., the entropy is low enough) to provide an accretion rate that is sufficient to power the AGN. The latter condition is probably met for low power jets (Allen et al. 2006). However, host galaxies of jets exceeding $\sim 10^{45}$ erg s $^{-1}$ would have great difficulty accreting enough hot fuel to power them (Rafferty et al. 2006; Hardcastle et al. 2007; McNamara et al. 2011). There are other difficulties. Bondi accretion is expected to operate without producing a substantial reservoir of cold gas. While this would be consistent with giant elliptical galaxies, it is at variance with the levels of cold gas found in BCGs (Edge 2001; Salomé & Combes 2003; Edge et al. 2010; Donahue et al. 2011; Ogle et al. 2010). If Bondi accretion is operating in low power AGN and cold accretion in high power AGN, the two feedback mechanisms must operate seamlessly on hot atmospheres spanning seven decades in jet power and X-ray luminosity. With rare exceptions, enough cold molecular gas is available in BCGs and probably in normal ellipticals to power their AGN (Edge 2001; Soker 2008). Sufficiency is no proof, but feeding the AGN with cold gas would obviate the need for two modes of accretion.

Further complicating matters, it remains unclear how the accretion rate for hot gas is affected by the small amount of angular momentum likely to be present (Narayan & Fabian 2011; Pizzolato & Soker 2010). Using 2-dimensional magnetohydrodynamic simulations, Proga & Begelman (2003) concluded that the accretion rate for slowly rotating hot gas could be orders of magnitude less than the Bondi accretion rate. In their model, angular momentum is transported outward by magnetorotational instability (MRI, Balbus & Hawley 1998). More recently, Inogamov & Sunyaev (2010) have made a hydrodynamic model for the accretion flow that includes thermal conduction and bremsstrahlung radiation losses. With no angular momentum transport, the “centrifugal barrier” plays a key role in this model, and it is no surprise that they also find accretion rates much smaller than the Bondi rate. By contrast, assuming a kinematic shear viscosity of the form $\alpha c_s r$, where c_s is the isothermal sound speed and r is the radius, Narayan & Fabian (2011) found that slowly rotating gas can accrete at close to the Bondi rate if $\alpha \sim 0.1$. The incompatibility of these results reflects widely differing physical assumptions concerning the transport of angular momentum. Their validity depends critically on the highly uncertain transport properties of the plasma, particularly the effective viscosity (section 5.5).

New evidence for a rising temperature gradient into the nucleus of NGC 3115 is consistent with Bondi flow (Wong et al. 2011), but it is also consistent with models having much lower accretion rates for the hot gas. For the Bondi accretion rate, \dot{M}_B , Wong et al.

(2011) estimate that the X-ray luminosity of the AGN in NGC 3115 is at least six orders of magnitude smaller than $0.1\dot{M}_B c^2$. That also makes the nuclear X-ray luminosity at least an order of magnitude smaller than the thermal power, $\dot{M}_B 5kT/(2\mu m_H)$, conveyed inward through the Bondi radius by the gas. If Bondi accretion does work, the radiative inefficiency of NGC 3115 is truly remarkable.

7.2. Black Hole Spin and AGN Feedback

A black hole’s spin encodes its formation history (Wilson & Colbert 1995; Moderski & Sikora 1996; Sikora et al. 2007; Volonteri & Stark 2011). A black hole growing by equal mass black hole mergers or during extended periods of prograde gas accretion is expected to be endowed with a high spin parameter (Volonteri et al. 2005). Black holes growing through the accretion of smaller black holes and by accretion of randomly-oriented gas disks are expected to have low spin parameters (King & Pringle 2006; King et al. 2008; Hughes & Blandford 2003; Gammie et al. 2004).

Like all astrophysical objects, black holes are almost certainly spinning. But estimates of their spin parameters are generally indirect and model dependent. A connection between a black hole’s rotation rate and its energetic output has been inferred from an apparent dichotomy between rapidly-spinning, radio loud AGN and slowly spinning, radio quiet AGN (Sikora et al. 2007; Martínez-Sansigre & Rawlings 2011; Wu et al. 2011). However, the association between instantaneous jet power and rotation rate depends on several factors including, the relationship between total radio power and its core radio luminosity, and the assumed black hole mass and its accretion disk geometry (Tchekhovskoy et al. 2010; Broderick & Fender 2011). In other words, only an indirect connection can be made between the angular momentum of a black hole and its emergent properties.¹ More direct estimates of black hole spin parameters have been obtained for several AGN using the shape and amplitude of the relativistically-broadened, 6.4 keV fluorescent iron feature. These measurements have generally revealed high spin parameters (Miller 2007; Tanaka et al. 1995; Fabian et al. 1995; Brenneman et al. 2011). In an exciting new development, long baseline millimeter interferometric observations are beginning to image the event horizon silhouettes in M87 and Sgr A* (Doeleman et al. 2008; Fish et al. 2011; Broderick et al. 2011). The spin parameter is derived from the structure of the silhouette. The initial results indicate rapidly and slowly spinning black holes for M87 and Sgr A*, respectively. Due to resolution limitations, this

¹A correlation between radio power and black hole spin was recently found for stellar mass black holes by Narayan & McClintock (2012).

method will be accessible only to M87 and Sgr A* for the foreseeable future.

Spin may play an important role in AGN feedback. The rotational energy of a maximally-spinning, $10^9 M_\odot$ black hole exceeds 10^{62} erg. This spin energy is significant with respect to the thermal energy of its surrounding X-ray atmosphere and is enough to quench a cooling flow for several Gyr. Under the right circumstances, the rotational energy may be released in the form of jets through the Penrose-Blandford-Znajek mechanism (Blandford & Znajek 1977; Hawley & Krolik 2006). The jetted outflow is coupled to the black hole’s rotational energy by magnetic fields supplied by and anchored to an accretion disk (Meier 1999; Beckwith et al. 2009; Krolik & Hawley 2010; Krolik et al. 2005). Tapping into spin to power a jet requires a significant level of accretion. The coupling between the angular momentum of the black hole and the accretion disk is weak for low spin parameters and may depend on whether the accretion disk is in pro- or retrograde rotation (Garofalo et al. 2010). It is unclear whether jet power is derived primarily from the spin itself or from the binding energy released by accretion. But in the context of feedback, it is accretion that must couple the rotational energy of the black hole to the feedback loop itself (McNamara et al. 2011).

We became interested in the possibility of coupling spin power to a feedback loop after noticing that some systems with extraordinarily powerful jets, such as those in the MS0735 cluster, are hosted by BCGs with relatively little cold gas (McNamara et al. 2009, 2011). If powered by accretion alone, MS0735’s $\sim 10^{62}$ erg AGN (Fig. 7) must have accreted at a rate of several solar masses per year for the $\sim 10^8$ yr duration of its outburst. This implies that its SMBH accreted several $10^8 M_\odot$ of gas. Yet its BCG harbors less than a few $10^9 M_\odot$ of cold gas (Salomé & Combes 2008) and shows no sign of star formation. If powered by accretion, an uncomfortably large fraction of its gas shed its angular momentum and was dispatched onto the black hole without forming stars. This scenario seems unrealistic. If the jets formed instead through a modified BZ process (Nemmen et al. 2007), even a rapidly-spinning, $10^9 M_\odot$ black hole would require a high accretion rate to power its jet, which is the scenario we hoped to avoid by appealing to spin. Note that accretion alone is unable to generate power above a few tens of percent of $\dot{M}c^2$. Therefore, an AGN substantially in excess of this limit must be powered by spin or by a process other than accretion.

A mechanism able to access the rotational energy of a SMBH efficiently and at low accretion rates, i.e., $P_{\text{jet}} > \dot{M}c^2$, may be needed to sustain the most powerful AGN (Ghisellini et al. 2010; Punsly 2011; Fernandes et al. 2011; McNamara et al. 2009, 2011). One such mechanism may be the magnetically arrested accretion model of Tchekhovskoy et al. (2011). Their model produced jet efficiencies exceeding 100%, i.e., $P_{\text{jet}} > \dot{M}c^2$, from a rapidly spinning SMBH at the center of a disk threaded by a large-scale poloidal magnetic field. High magnetic field pressure is sustained in part by ram pressure from accreting gas (see also Cao

2011; McKinney et al. 2012). Accreting matter presses the poloidal disk field into the ergosphere, maximizing energy yield via the Blandford-Znajek mechanism. It has been reasoned that shear in the disk causes the toroidal component of the field to dominate anywhere close to the black hole. In particular, if accretion is governed by turbulent viscosity generated by MRI (Balbus & Hawley 1998; De Villiers et al. 2003), a large-scale poloidal field seems unlikely. However, poor understanding of the accretion process leaves plenty of room for a mechanism to obtain strong poloidal fields. Such a mechanism is more plausible for hot, pressure supported, quasi-spherical accretion flows than for cold accretion through a thin disk.

Spinning black holes launch Poynting flux jets along the black hole’s spin axis (Nakamura et al. 2008) that carry very little matter with them (Hawley & Krolik 2006). Using the distribution of X-ray cavity sizes as a function of their distance from the nucleus, Diehl et al. (2008) argued that their size distribution is consistent with predictions for Poynting jets but not for adiabatically expanding hydrodynamic cavities. On the other hand, the large jet powers inferred from X-ray cavities require energetic protons or other heavy particles to maintain pressure balance. If jets are dominated by Poynting flux on small scales, they must undergo significant mass loading before reaching the radio lobes.

8. AGN Heating in Distant Clusters

Most of what we have learned about AGN heating is based on X-ray observations of bright, nearby clusters that are much easier to observe. Atmospheric heating by AGN is expected to become increasingly important in distant clusters as AGN activity rises. The excess entropy in hot atmospheres (Voit 2005; Pfrommer et al. 2011) may be the relic of primeval heating by AGN and star formation (Kaiser 1991). But whether the excess entropy was injected in an early “preheating” phase (Kaiser 1991) or more gradually over time is unknown. Systematic studies of atmospheric heating in distant clusters are needed to address this issue.

Examples of the few targeted studies of distant cavity systems are the $z = 0.35$ clusters RBS 797 (Schindler et al. 2001; Cavagnolo et al. 2011, and Doria et al. in preparation) and MACSJ1931.8-2634 (Ehlert et al. 2011). Both have AGN mechanical powers in the range $10^{45} - 10^{46}$ ergs $^{-1}$. The MACSJ1931 BCG (Ehlert et al. 2011) is a spectacular galaxy with knots of star formation, nebular emission, radio jets, and X-ray cavities (Fig. 14). After accounting for AGN heating, its star formation and cooling rates at $170 M_{\odot} \text{ yr}^{-1}$ are both consistent with each other. This is a solid example of a burgeoning BCG that may be regulated by AGN feedback. Hlavacek-Larrondo et al. (2011) examined the prevalence of

X-ray cavities in a sample of 83 MACS clusters lying in the redshift range $z = 0.3 - 0.7$. They found no evolution in the average jet power or cavity properties over their sample. This study shows that radio-AGN feedback was operating on cooling flows in the most massive clusters when the Universe was nearly half its current age as it is operating today.

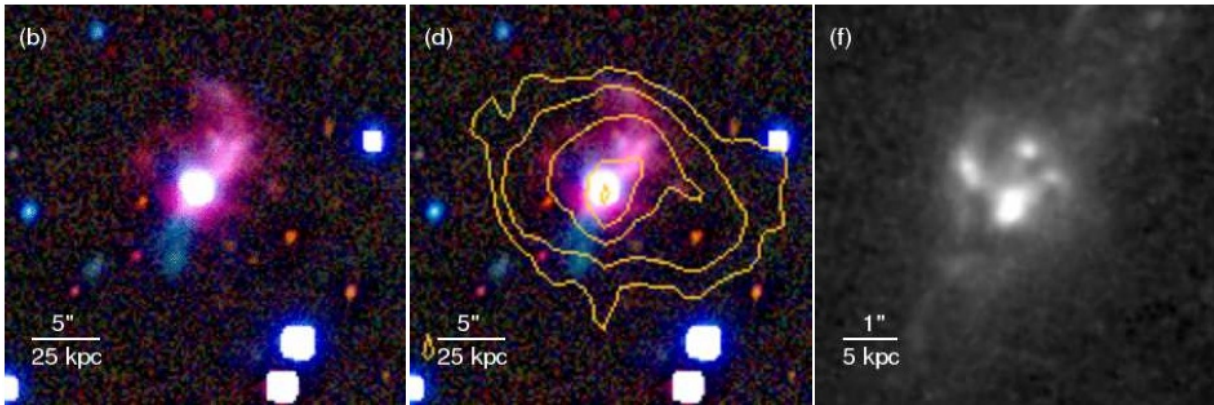


Fig. 14.— Optical structure of the BCG of MACS J1931.8-2634. SuprimeCam BRz image of the central 30 arcsec by 30 arcsec. (b): the contribution from the old stellar population of the BCG (as traced by the SuprimeCam I-band image) was subtracted from each of the B,R and z images before combining them to create a color image. This enhances the blue and pink features visible to the southeast and northwest of the central AGN. Pink signals contributions from predominantly the blue (B) and the red (z) channel. At the redshift of the cluster, the $H\alpha$ line falls into the z-band, and thus this emission likely stems from $H\alpha$ nebulosity surrounding MACS J1931.8-2634. The blue emission signals a young stellar population (d): Overlay of the radio emission on (b). (f): The central 7.5 arcsec by 7.5 arcsec of an HST snapshot. Note the bright knots in a spiral-like structure emanating to the Northwest of the brightest central knot (Ehlert et al. 2011).

Other studies of AGN heating beyond a redshift of 0.3 have approached this problem statistically. Most have focussed on the detection frequency of AGN in the general population of galaxies in clusters (Martini et al. 2002, 2009; Eastman et al. 2007; Galametz et al. 2009). These studies found a dramatic increase in the numbers of X-ray and infrared-emitting AGN in galaxies projected within clusters out to and beyond redshift one. This increase reflects the universal rise of AGN activity with increasing redshift, but it does not probe atmospheric heating because radiation couples weakly to the keV gas.

Radio AGN are strongly coupled to the keV gas and are thus able to probe atmospheric heating. Radio AGN in clusters lying within $z \sim 1$ tend to be centrally concentrated and are more numerous than X-ray and infrared AGN (Best et al. 2007; Galametz et al. 2009).

Galametz et al. (2009) and Ma et al. (2011) found that the detection fraction of radio AGN rises with redshift by less than a factor of two in the range $z \sim 0.2 - 1$, while the numbers of X-ray AGN rise dramatically over this redshift range (Galametz et al. 2009). Hart et al. (2009, 2011) measured the incidence of radio AGN in a dozen X-ray clusters in the range $z \sim 0.4 - 1.2$, specifically chosen to match Coma-like progenitors. They found roughly 17 cluster radio galaxies in their sample within a projected radius of 1 Mpc from the cluster centers. Unlike Galametz et al. (2009) and Ma et al. (2011), Hart et al. (2011) found strong redshift evolution of the cluster radio luminosity function, consistent with a near tenfold increase in the AGN heating rate by galaxies throughout clusters at a redshift of one compared to today.

Ma et al. (2011) cross correlated the NVSS radio catalog with 242 clusters from the 400 Square Degree X-ray cluster catalog (Burenin et al. 2007). Their clusters lie within the redshift range $0.2 < z < 0.7$ and have bolometric X-ray luminosities of $10^{43} < L_x < 10^{45}$ erg s⁻¹. Ma found a high incidence of radio galaxies within a projected radius of 250 kpc indicating that AGN heating is probably significant. Using scaling relations between radio luminosity and cavity power (Birzan et al. 2008; Cavagnolo et al. 2010), Ma et al. found that the integrated AGN power over this luminosity range is nearly constant and independent of cluster X-ray luminosity. Only a mild, perhaps two-fold increase in average jet power is seen between $0.15 < z < 0.6$, which is consistent with the results of Galametz et al. (2009). The key result is that the ratio of jet power to X-ray luminosity increases fourfold, from roughly 1/2 in the most luminous, $L_x \sim 10^{45}$ erg s⁻¹, clusters to $\simeq 2$ in lower luminosity, $L_x \sim 5 \times 10^{43}$ erg s⁻¹, clusters. The relatively constant AGN power input with X-ray luminosity implies that AGN heating is more effective in lower luminosity clusters containing fewer gas particles than high luminosity clusters. AGN heating in groups may be more dramatic, in some cases sweeping away their hot atmospheres (Giodini et al. 2010). Finally, radio AGN heating of the hot atmospheres of elliptical galaxies was apparently operating at $z \sim 1.2$ as it is today (Danielson et al. 2012).

Assuming no evolution, Ma et al. (2011) found an average energy input of approximately 0.2 keV per baryon within R_{500} . This value would double if the integrated jet power remained constant out to $z = 2$, and would increase even more if the radio luminosity function increases in clusters at higher redshifts. More recent work by Ma and collaborators studying a much larger sample of X-ray clusters indicates that AGN heating approaches ~ 1 keV per baryon in low luminosity clusters. AGN heating would then be significant compared to the ~ 1 keV per baryon needed to explain the excess entropy in clusters (Kaiser 1991; Wu et al. 2000; Voit 2005). These studies taken together imply that gradual heating over time may be as important or more important than Kaiser’s early preheating scenario (cf. Young et al. 2011).

8.1. Are Strong Cooling Flows in Ascendency?

A potential consequence of AGN heating in distant clusters would be the growing, albeit tentative, evidence for a decline in the frequency of *strong* cooling cores (flows) in distant clusters. Despite an expected tendency for X-ray-selected clusters to be biased in favor of bright, cooling cores (Eckert et al. 2011), distant clusters in the 400SD, WARPS, and RDCS surveys lack the large numbers of bright central cusps of X-ray emission associated with cooling flows in nearby samples (Vikhlinin et al. 2007; Santos et al. 2010), such as the *ROSAT* All Sky Survey (Crawford et al. 1999a). Bolstering this finding, the incidence of radio loud BCGs in 400SD clusters is roughly 30% (Ma et al. 2011), a rate that is consistent with the detection fraction of relatively normal Sloan clusters (Best et al. 2007), but far below the 70% – 90% detection rate in strong cooling flow clusters (Burns 1990; Best et al. 2007; Cavagnolo et al. 2008; Mittal et al. 2009; Dunn & Fabian 2008).

The radio detection rate found by Ma et al. (2011) is consistent with the absence of *strong* cooling flows in distant 400 Square Degree X-ray clusters, but not inconsistent with significant numbers of smaller cooling flows. A similar conclusion was reached by Samuele et al. (2011), who found that strong nebular line emission features were absent in 77 BCGs selected from the 160SD cluster survey. Nebular emission is a reliable indicator of the presence of a cooling flow (Cowie et al. 1983; Heckman et al. 1989; Donahue et al. 1992; Crawford et al. 1999a; McDonald et al. 2010), yet Samuele et al. (2011) found their numbers declining at redshifts 0.3 – 0.5. The Samuele et al. (2011) result was recently confirmed by McDonald (2011) using a different sample of clusters.

These studies do not preclude the existence of moderate to weak cooling flows in distant clusters. But they are consistent with declining numbers of *strong*, Perseus-like cooling flows at higher redshift. Andy Fabian has suggested to us that this decline may reflect the bias against the X-ray detection of cooling flow clusters hosting central X-ray-bright quasars that outshine the thermal emission from the surrounding cluster (e.g., Russell et al. 2010; Siemiginowska et al. 2010). This must be happening at some level. But the numbers of X-ray-bright AGN in distant BCGs are unlikely to be high enough to account for this effect. Although selection effects are always an issue (e.g., Santos et al. 2010), the evidence for declining numbers of strong cooling flows beyond redshift ~ 0.3 is growing and is probably real.

9. Concluding Remarks

A strong empirical case has emerged in recent years that AGN feedback limits gas cooling and star formation in the cores of low redshift galaxy clusters and groups. The impact of AGN outbursts on cluster atmospheres is evident in high resolution X-ray images. They displace gas, drive shocks and sound waves, and they transport low entropy gas and heavy elements outward from cluster cores. AGN in BCGs also respond to their environments with a higher incidence of radio activity and greater jet powers in richer clusters. The average mechanical power output adjusts to the level required to inhibit gas from cooling and forming stars. While cooling hot gas may not be the only cause of AGN activity in BCGs, it is clearly implicated as a significant factor. Star formation and cool gas are found exclusively in BCGs located in cluster cores with the shortest cooling times that are most prone to thermal instability.

Understanding of the AGN mechanical feedback loop lags the observational evidence for it. A number of processes have been identified that can play some role in dissipating and distributing outburst energy in hosting atmospheres, but it remains unclear which of them are most significant. Perhaps the greatest obstacle to progress here is poor understanding of transport processes. Certainly, anisotropic transport due to magnetic fields must be taken into account, but it is possible that transport and dissipation in the intracluster plasma are no less complex than they are in the solar wind plasma, in which case existing models are inadequate. Further work is required to clarify this issue.

Bondi accretion could power most AGN outbursts observed locally, but small angular momentum may cause a drastic reduction in accretion rates, another issue remaining to be resolved. There is a small number of systems in which the fuel supply from Bondi accretion is insufficient to power the jets. Large quantities of cold gas found in many systems might provide an alternative source of fuel in those cases. It remains to be determined which source of fuel, hot gas or cooled hot gas, is mainly responsible for powering mechanical feedback in BCGs. Furthermore, the enormous energies of some outbursts challenge all accretion powered models, suggesting that black hole spin may need to be tapped as the energy source in at least some cases. General relativistic magnetohydrodynamical simulations are just beginning to shed light on this issue.

Observations with *Chandra* and *XMM-Newton* have been critical to progress in this field so far. In the near future, it will be possible to address many of the open questions with a suite of new instruments. The planned X-ray survey of *eROSITA* will provide a census of systems with extended hot atmospheres, including large samples of galaxy clusters at redshifts beyond one. Many of these and other nearby bright clusters will be observed with the microcalorimeter array on the ASTRO-H observatory, hopefully revealing the level

of turbulence in the hot gas produced by AGN outflows and other processes. The *eROSITA* survey will be complemented by forthcoming radio surveys. Notably, the planned ASKAP EMU and Westerbork Wodan surveys will cover the full radio sky at ~ 1 GHz, with much greater sensitivity and spatial resolution than the existing NVSS. At lower radio frequencies, LOFAR will be an excellent tool for studying older radio outbursts that have faded at higher radio frequencies. Surveys by these instruments will be particularly valuable for studying mechanical outbursts from AGN at redshifts of one and beyond to investigate the history of mechanical feedback during the formation of groups and clusters. They will also provide data on mechanical feedback in the era when the radiation powered quasar mode of AGN feedback is thought to have played a much greater role than it does today. The high sensitivity and angular resolution of ALMA will enable detailed studies of the distribution and dynamics of cold gas in elliptical galaxies, and the relative importance of star formation and starburst winds in regulating the flow of gas onto the nucleus. These exciting new measurements will help to constrain the origin, perhaps as cooled hot gas, and fate of the molecular gas, in star formation and fueling AGN. Measurements of gas dynamics with ALMA will also provide much better constraints on black hole masses in elliptical galaxies, hence their Bondi and Eddington accretion rates.

We thank Helen Russell, Massimo Gaspari, Christoph Pfrommer, Prateek Sharma, Bill Mathews and especially Mark Voit and Peter Mendygral for their help and advice. This work was supported in part by NASA contract NAS8-03060, Chandra Large Project Grant GO9-0140X, and generous funding from the Natural Sciences and Engineering Research Council of Canada, and an SSEP grant from the Canadian Space Agency.

REFERENCES

- Alexander, D. M. & Hickox, R. C. 2011, ArXiv e-prints
- Alexander, D. M., Swinbank, A. M., Smail, I., McDermid, R., & Nesvadba, N. P. H. 2010, MNRAS, 402, 2211
- Allen, S. W., Dunn, R. J. H., Fabian, A. C., Taylor, G. B., & Reynolds, C. S. 2006, MNRAS, 372, 21
- Allen, S. W., Evrard, A. E., & Mantz, A. B. 2011, ArXiv e-prints
- Allen, S. W. & Fabian, A. C. 1998, MNRAS, 297, L63

- Arnaud, M., Rothenflug, R., Boulade, O., Vigroux, L., & Vangioni-Flam, E. 1992, *A&A*, 254, 49
- Balbus, S. A. 2000, *ApJ*, 534, 420
- Balbus, S. A. & Hawley, J. F. 1998, *Reviews of Modern Physics*, 70, 1
- Baldry, I. K., Glazebrook, K., Brinkmann, J., Ivezić, Ž., Lupton, R. H., Nichol, R. C., & Szalay, A. S. 2004, *ApJ*, 600, 681
- Balogh, M. L., Pearce, F. R., Bower, R. G., & Kay, S. T. 2001, *MNRAS*, 326, 1228
- Baugh, C. M. 2006, *Reports on Progress in Physics*, 69, 3101
- Baum, S. A. & O’Dea, C. P. 1991, *MNRAS*, 250, 737
- Beckwith, K., Hawley, J. F., & Krolik, J. H. 2009, *ApJ*, 707, 428
- Begelman, M. C., Blandford, R. D., & Rees, M. J. 1984, *Reviews of Modern Physics*, 56, 255
- Best, P. N., Kaiser, C. R., Heckman, T. M., & Kauffmann, G. 2006, *MNRAS*, 368, L67
- Best, P. N., von der Linden, A., Kauffmann, G., Heckman, T. M., & Kaiser, C. R. 2007, *MNRAS*, 379, 894
- Bildfell, C., Hoekstra, H., Babul, A., & Mahdavi, A. 2008, *MNRAS*, 389, 1637
- Binney, J. & Tabor, G. 1995, *MNRAS*, 276, 663
- Birnboim, Y. & Dekel, A. 2011, *MNRAS*, 415, 2566
- Bîrzan, L., McNamara, B. R., Nulsen, P. E. J., Carilli, C. L., & Wise, M. W. 2008, *ApJ*, 686, 859
- Bîrzan, L., Rafferty, D. A., McNamara, B. R., Wise, M. W., & Nulsen, P. E. J. 2004, *ApJ*, 607, 800
- Blandford, R. D. & Begelman, M. C. 1999, *MNRAS*, 303, L1
- Blandford, R. D. & Znajek, R. L. 1977, *MNRAS*, 179, 433
- Blanton, E. L., Clarke, T. E., Sarazin, C. L., Randall, S. W., & McNamara, B. R. 2010, *Proceedings of the National Academy of Science*, 107, 7174

- Blanton, E. L., Randall, S. W., Clarke, T. E., Sarazin, C. L., McNamara, B. R., Douglass, E. M., & McDonald, M. 2011, *ApJ*, 737, 99
- Blanton, E. L., Sarazin, C. L., & McNamara, B. R. 2003, *ApJ*, 585, 227
- Boehringer, H. & Morfill, G. E. 1988, *ApJ*, 330, 609
- Boehringer, H., Voges, W., Fabian, A. C., Edge, A. C., & Neumann, D. M. 1993, *MNRAS*, 264, L25
- Bogdanović, T., Reynolds, C. S., Balbus, S. A., & Parrish, I. J. 2009, *ApJ*, 704, 211
- Bonafede, A., Govoni, F., Feretti, L., Murgia, M., Giovannini, G., & Brüggén, M. 2011, *A&A*, 530, A24
- Borgani, S., Fabjan, D., Tornatore, L., Schindler, S., Dolag, K., & Diaferio, A. 2008, *Space Sci. Rev.*, 134, 379
- Borgani, S. & Kravtsov, A. 2009, *astro-ph/0906.4370*
- Bower, R. G., Benson, A. J., Malbon, R., Helly, J. C., Frenk, C. S., Baugh, C. M., Cole, S., & Lacey, C. G. 2006, *MNRAS*, 370, 645
- Bower, R. G., McCarthy, I. G., & Benson, A. J. 2008, *MNRAS*, 390, 1399
- Braginskii, S. I. 1965, *Reviews of Plasma Physics*, 1, 205
- Bregman, J. N. 2007, *ARA&A*, 45, 221
- Bregman, J. N. & David, L. P. 1988, *ApJ*, 326, 639
- Brenneman, L. W., Reynolds, C. S., Nowak, M. A., Reis, R. C., Trippe, M., Fabian, A. C., Iwasawa, K., Lee, J. C., Miller, J. M., Mushotzky, R. F., Nandra, K., & Volonteri, M. 2011, *ApJ*, 736, 103
- Broderick, A. E., Loeb, A., & Reid, M. J. 2011, *ApJ*, 735, 57
- Broderick, J. W. & Fender, R. P. 2011, *MNRAS*, 417, 184
- Brüggén, M. & Kaiser, C. R. 2002, *Nature*, 418, 301
- Brüggén, M., Ruszkowski, M., & Hallman, E. 2005, *ApJ*, 630, 740
- Burenin, R. A., Vikhlinin, A., Hornstrup, A., Ebeling, H., Quintana, H., & Mescheryakov, A. 2007, *ApJS*, 172, 561

- Burns, J. O. 1990, *AJ*, 99, 14
- Cao, X. 2011, *ApJ*, 737, 94
- Carilli, C. L., Perley, R. A., & Harris, D. E. 1994, *MNRAS*, 270, 173
- Carilli, C. L. & Taylor, G. B. 2002, *ARA&A*, 40, 319
- Cattaneo, A., Faber, S. M., Binney, J., Dekel, A., Kormendy, J., Mushotzky, R., Babul, A., Best, P. N., Brüggen, M., Fabian, A. C., Frenk, C. S., Khalatyan, A., Netzer, H., Mahdavi, A., Silk, J., Steinmetz, M., & Wisotzki, L. 2009, *Nature*, 460, 213
- Cavagnolo, K. W., Donahue, M., Voit, G. M., & Sun, M. 2008, *ApJ*, 683, L107
- . 2009, *ApJS*, 182, 12
- Cavagnolo, K. W., McNamara, B. R., Nulsen, P. E. J., Carilli, C. L., Jones, C., & Bîrzan, L. 2010, *ApJ*, 720, 1066
- Cavagnolo, K. W., McNamara, B. R., Wise, M. W., Nulsen, P. E. J., Brüggen, M., Gitti, M., & Rafferty, D. A. 2011, *ApJ*, 732, 71
- Chartas, G., Brandt, W. N., Gallagher, S. C., & Proga, D. 2007, *AJ*, 133, 1849
- Churazov, E., Brüggen, M., Kaiser, C. R., Böhringer, H., & Forman, W. 2001, *ApJ*, 554, 261
- Churazov, E., Sazonov, S., Sunyaev, R., Forman, W., Jones, C., & Böhringer, H. 2005, *MNRAS*, 363, L91
- Churazov, E., Sunyaev, R., Forman, W., & Böhringer, H. 2002, *MNRAS*, 332, 729
- Cowie, L. L., Hu, E. M., Jenkins, E. B., & York, D. G. 1983, *ApJ*, 272, 29
- Crawford, C. S., Allen, S. W., Ebeling, H., Edge, A. C., & Fabian, A. C. 1999a, *MNRAS*, 306, 857
- Crawford, C. S., Lehmann, I., Fabian, A. C., Bremer, M. N., & Hasinger, G. 1999b, *MNRAS*, 308, 1159
- Croston, J. H. 2008, in *Astronomical Society of the Pacific Conference Series*, Vol. 386, *Extragalactic Jets: Theory and Observation from Radio to Gamma Ray*, ed. T. A. Rector & D. S. De Young, 335–+

- Croston, J. H., Kraft, R. P., Hardcastle, M. J., Birkinshaw, M., Worrall, D. M., Nulsen, P. E. J., Penna, R. F., Sivakoff, G. R., Jordán, A., Brassington, N. J., Evans, D. A., Forman, W. R., Gilfanov, M., Goodger, J. L., Harris, W. E., Jones, C., Juett, A. M., Murray, S. S., Raychaudhury, S., Sarazin, C. L., Voss, R., & Woodley, K. A. 2009, *MNRAS*, 395, 1999
- Croton, D. J., Springel, V., White, S. D. M., De Lucia, G., Frenk, C. S., Gao, L., Jenkins, A., Kauffmann, G., Navarro, J. F., & Yoshida, N. 2006, *MNRAS*, 365, 11
- Danielson, A. L. R., Lehmer, B. D., Alexander, D. M., Brandt, W. N., Luo, B., Miller, N., Xue, Y. Q., & Stott, J. P. 2012, *ArXiv e-prints*
- Davé, R., Cen, R., Ostriker, J. P., Bryan, G. L., Hernquist, L., Katz, N., Weinberg, D. H., Norman, M. L., & O’Shea, B. 2001, *ApJ*, 552, 473
- Davé, R., Finlator, K., & Oppenheimer, B. D. 2011a, *ArXiv e-prints*
- Davé, R., Oppenheimer, B. D., & Finlator, K. 2011b, *MNRAS*, 415, 11
- David, L. P., Jones, C., Forman, W., Nulsen, P., Vrtilik, J., O’Sullivan, E., Giacintucci, S., & Raychaudhury, S. 2009, *ApJ*, 705, 624
- David, L. P. & Nulsen, P. E. J. 2008, *ApJ*, 689, 837
- David, L. P., Nulsen, P. E. J., McNamara, B. R., Forman, W., Jones, C., Ponman, T., Robertson, B., & Wise, M. 2001, *ApJ*, 557, 546
- Davis, M., Efstathiou, G., Frenk, C. S., & White, S. D. M. 1985, *ApJ*, 292, 371
- De Grandi, S., Ettori, S., Longhetti, M., & Molendi, S. 2004, *A&A*, 419, 7
- De Grandi, S. & Molendi, S. 2001, *ApJ*, 551, 153
- de Kool, M., Arav, N., Becker, R. H., Gregg, M. D., White, R. L., Laurent-Muehleisen, S. A., Price, T., & Korista, K. T. 2001, *ApJ*, 548, 609
- de Plaa, J., Werner, N., Bleeker, J. A. M., Vink, J., Kaastra, J. S., & Méndez, M. 2007, *A&A*, 465, 345
- De Villiers, J.-P., Hawley, J. F., & Krolik, J. H. 2003, *ApJ*, 599, 1238
- De Young, D. S. 2006, *ApJ*, 648, 200
- . 2010, *ApJ*, 710, 743

- Dennis, T. J. & Chandran, B. D. G. 2005, *ApJ*, 622, 205
- Di Matteo, T., Springel, V., & Hernquist, L. 2005, *Nature*, 433, 604
- Diehl, S., Li, H., Fryer, C. L., & Rafferty, D. 2008, *ApJ*, 687, 173
- Doeleman, S. S., Weintroub, J., Rogers, A. E. E., Plambeck, R., Freund, R., Tilanus, R. P. J., Friberg, P., Ziurys, L. M., Moran, J. M., Corey, B., Young, K. H., Smythe, D. L., Titus, M., Marrone, D. P., Cappallo, R. J., Bock, D. C.-J., Bower, G. C., Chamberlin, R., Davis, G. R., Krichbaum, T. P., Lamb, J., Maness, H., Niell, A. E., Roy, A., Strittmatter, P., Werthimer, D., Whitney, A. R., & Woody, D. 2008, *Nature*, 455, 78
- Donahue, M., Bruch, S., Wang, E., Voit, G. M., Hicks, A. K., Haarsma, D. B., Croston, J. H., Pratt, G. W., Pierini, D., O’Connell, R. W., & Böhringer, H. 2010, *ApJ*, 715, 881
- Donahue, M., de Messières, G. E., O’Connell, R. W., Voit, G. M., Hoffer, A., McNamara, B. R., & Nulsen, P. E. J. 2011, *ApJ*, 732, 40
- Donahue, M., Stocke, J. T., & Gioia, I. M. 1992, *ApJ*, 385, 49
- Dong, R., Rasmussen, J., & Mulchaey, J. S. 2010, *ApJ*, 712, 883
- Dunn, R. J. H. & Fabian, A. C. 2006, *MNRAS*, 373, 959
- . 2008, *MNRAS*, 385, 757
- Dunn, R. J. H., Fabian, A. C., & Sanders, J. S. 2006, *MNRAS*, 366, 758
- Dupke, R. A. & White, III, R. E. 2000, *ApJ*, 537, 123
- Eastman, J., Martini, P., Sivakoff, G., Kelson, D. D., Mulchaey, J. S., & Tran, K.-V. 2007, *ApJ*, 664, L9
- Eckert, D., Molendi, S., & Paltani, S. 2011, *A&A*, 526, A79+
- Edge, A. C. 2001, *MNRAS*, 328, 762
- Edge, A. C. & Frayer, D. T. 2003, *ApJ*, 594, L13
- Edge, A. C., Oonk, J. B. R., Mittal, R., Allen, S. W., Baum, S. A., Böhringer, H., Bregman, J. N., Bremer, M. N., Combes, F., Crawford, C. S., Donahue, M., Egami, E., Fabian, A. C., Ferland, G. J., Hamer, S. L., Hatch, N. A., Jaffe, W., Johnstone, R. M., McNamara, B. R., O’Dea, C. P., Popesso, P., Quillen, A. C., Salomé, P., Sarazin, C. L., Voit, G. M., Wilman, R. J., & Wise, M. W. 2010, *A&A*, 518, L46+

- Ehlert, S., Allen, S. W., von der Linden, A., Simionescu, A., Werner, N., Taylor, G. B., Gentile, G., Ebeling, H., Allen, M. T., Applegate, D., Dunn, R. J. H., Fabian, A. C., Kelly, P., Million, E. T., Morris, R. G., Sanders, J. S., & Schmidt, R. W. 2011, *MNRAS*, 411, 1641
- Enßlin, T., Pfrommer, C., Miniati, F., & Subramanian, K. 2011, *A&A*, 527, A99
- Fabian, A. C. 1994, *ARA&A*, 32, 277
- Fabian, A. C., Nandra, K., Reynolds, C. S., Brandt, W. N., Otani, C., Tanaka, Y., Inoue, H., & Iwasawa, K. 1995, *MNRAS*, 277, L11
- Fabian, A. C., Nulsen, P. E. J., & Canizares, C. R. 1982, *MNRAS*, 201, 933
- Fabian, A. C. & Rees, M. J. 1995, *MNRAS*, 277, L55
- Fabian, A. C., Reynolds, C. S., Taylor, G. B., & Dunn, R. J. H. 2005a, *MNRAS*, 363, 891
- Fabian, A. C., Sanders, J. S., Allen, S. W., Canning, R. E. A., Churazov, E., Crawford, C. S., Forman, W., GaBany, J., Hlavacek-Larrondo, J., Johnstone, R. M., Russell, H. R., Reynolds, C. S., Salome, P., Taylor, G. B., & Young, A. J. 2011, *astro-ph/1105.5025*
- Fabian, A. C., Sanders, J. S., Allen, S. W., Crawford, C. S., Iwasawa, K., Johnstone, R. M., Schmidt, R. W., & Taylor, G. B. 2003a, *MNRAS*, 344, L43
- Fabian, A. C., Sanders, J. S., Crawford, C. S., Conselice, C. J., Gallagher, J. S., & Wyse, R. F. G. 2003b, *MNRAS*, 344, L48
- Fabian, A. C., Sanders, J. S., Taylor, G. B., & Allen, S. W. 2005b, *MNRAS*, 360, L20
- Fabjan, D., Borgani, S., Tornatore, L., Saro, A., Murante, G., & Dolag, K. 2010, *MNRAS*, 401, 1670
- Falcke, H., Körding, E., & Markoff, S. 2004, *A&A*, 414, 895
- Fender, R., Corbel, S., Tzioumis, T., McIntyre, V., Campbell-Wilson, D., Nowak, M., Sood, R., Hunstead, R., Harmon, A., Durouchoux, P., & Heindl, W. 1999, *ApJ*, 519, L165
- Fernandes, C. A. C., Jarvis, M. J., Rawlings, S., Martínez-Sansigre, A., Hatziminaoglou, E., Lacy, M., Page, M. J., Stevens, J. A., & Vardoulaki, E. 2011, *MNRAS*, 411, 1909
- Finlator, K. & Davé, R. 2008, *MNRAS*, 385, 2181

- Fish, V. L., Doeleman, S. S., Beaudoin, C., Blundell, R., Bolin, D. E., Bower, G. C., Chamberlin, R., Freund, R., Friberg, P., Gurwell, M. A., Honma, M., Inoue, M., Krichbaum, T. P., Lamb, J., Marrone, D. P., Moran, J. M., Oyama, T., Plambeck, R., Primiani, R., Rogers, A. E. E., Smythe, D. L., SooHoo, J., Strittmatter, P., Tilanus, R. P. J., Titus, M., Weintroub, J., Wright, M., Woody, D., Young, K. H., & Ziurys, L. M. 2011, *ApJ*, 727, L36+
- Forman, W., Jones, C., Churazov, E., Markevitch, M., Nulsen, P., Vikhlinin, A., Begelman, M., Böhringer, H., Eilek, J., Heinz, S., Kraft, R., Owen, F., & Pahre, M. 2007, *ApJ*, 665, 1057
- Forman, W., Nulsen, P., Heinz, S., Owen, F., Eilek, J., Vikhlinin, A., Markevitch, M., Kraft, R., Churazov, E., & Jones, C. 2005, *ApJ*, 635, 894
- Gabor, J. M., Davé, R., Oppenheimer, B. D., & Finlator, K. 2011, *MNRAS*, 417, 2676
- Galametz, A., Stern, D., Eisenhardt, P. R. M., Brodwin, M., Brown, M. J. I., Dey, A., Gonzalez, A. H., Jannuzi, B. T., Moustakas, L. A., & Stanford, S. A. 2009, *ApJ*, 694, 1309
- Gammie, C. F., Shapiro, S. L., & McKinney, J. C. 2004, *ApJ*, 602, 312
- Garofalo, D., Evans, D. A., & Sambruna, R. M. 2010, *MNRAS*, 406, 975
- Gaspari, M., Brighenti, F., D’Ercole, A., & Melioli, C. 2011a, *MNRAS*, 415, 1549
- Gaspari, M., Melioli, C., Brighenti, F., & D’Ercole, A. 2011b, *MNRAS*, 411, 349
- Gaspari, M., Ruszkowski, M., & Sharma, P. 2011c, *ArXiv e-prints*
- Ghisellini, G., Tavecchio, F., Foschini, L., Ghirlanda, G., Maraschi, L., & Celotti, A. 2010, *MNRAS*, 402, 497
- Giacintucci, S., O’Sullivan, E., Vrtilek, J., David, L. P., Raychaudhury, S., Venturi, T., Athreya, R. M., Clarke, T. E., Murgia, M., Mazzotta, P., Gitti, M., Ponman, T., Ishwara-Chandra, C. H., Jones, C., & Forman, W. R. 2011, *ApJ*, 732, 95
- Giodini, S., Smolčić, V., Finoguenov, A., Böhringer, H., Bîrzan, L., Zamorani, G., Oklopčić, A., Pierini, D., Pratt, G. W., Schinnerer, E., Massey, R., Koekemoer, A. M., Salvato, M., Sanders, D. B., Kartaltepe, J. S., & Thompson, D. 2010, *ApJ*, 714, 218
- Gitti, M., Brighenti, F., & McNamara, B. R. 2011a, *ArXiv e-prints*
- Gitti, M., McNamara, B. R., Nulsen, P. E. J., & Wise, M. W. 2007, *ApJ*, 660, 1118

- Gitti, M., Nulsen, P. E. J., David, L. P., McNamara, B. R., & Wise, M. W. 2011b, *ApJ*, 732, 13
- Gitti, M., O’Sullivan, E., Giacintucci, S., David, L. P., Vrtilik, J., Raychaudhury, S., & Nulsen, P. E. J. 2010, *ApJ*, 714, 758
- Guo, F. & Mathews, W. G. 2010, *ApJ*, 717, 937
- Guo, F. & Oh, S. P. 2008, *MNRAS*, 384, 251
- Hardcastle, M. J. & Croston, J. H. 2010, *MNRAS*, 404, 2018
- Hardcastle, M. J., Evans, D. A., & Croston, J. H. 2007, *MNRAS*, 376, 1849
- Hart, Q. N., Stocke, J. T., Evrard, A. E., Ellingson, E. E., & Barkhouse, W. A. 2011, [astro-ph/1107.1867](https://arxiv.org/abs/1107.1867)
- Hart, Q. N., Stocke, J. T., & Hallman, E. J. 2009, *ApJ*, 705, 854
- Hawley, J. F. & Krolik, J. H. 2006, *ApJ*, 641, 103
- Haynes, M. P., Brown, R. L., & Roberts, M. S. 1978, *ApJ*, 221, 414
- Heckman, T. M. 1981, *ApJ*, 250, L59
- Heckman, T. M., Armus, L., & Miley, G. K. 1990, *ApJS*, 74, 833
- Heckman, T. M., Baum, S. A., van Breugel, W. J. M., & McCarthy, P. 1989, *ApJ*, 338, 48
- Heckman, T. M., Lehnert, M. D., Strickland, D. K., & Armus, L. 2000, *ApJS*, 129, 493
- Heinz, S., Brüggem, M., Young, A., & Levesque, E. 2006, *MNRAS*, 373, L65
- Heinz, S. & Churazov, E. 2005, *ApJ*, 634, L141
- Hickox, R. C., Jones, C., Forman, W. R., Murray, S. S., Kochanek, C. S., Eisenstein, D., Jannuzi, B. T., Dey, A., Brown, M. J. I., Stern, D., Eisenhardt, P. R., Gorjian, V., Brodwin, M., Narayan, R., Cool, R. J., Kenter, A., Caldwell, N., & Anderson, M. E. 2009, *ApJ*, 696, 891
- Hicks, A. K., Mushotzky, R., & Donahue, M. 2010, *ApJ*, 719, 1844
- Hlavacek-Larrondo, J. & Fabian, A. C. 2011, *MNRAS*, 413, 313
- Hlavacek-Larrondo, J., Fabian, A. C., Edge, A. C., Ebeling, H., Sanders, J. S., Hogan, M. T., & Taylor, G. B. 2011, [ArXiv e-prints](https://arxiv.org/abs/1107.1867)

- Hu, E. M., Cowie, L. L., & Wang, Z. 1985, *ApJS*, 59, 447
- Hudson, D. S., Mittal, R., Reiprich, T. H., Nulsen, P. E. J., Andernach, H., & Sarazin, C. L. 2010, *A&A*, 513, A37
- Hughes, S. A. & Blandford, R. D. 2003, *ApJ*, 585, L101
- Inogamov, N. A. & Sunyaev, R. A. 2010, *Astronomy Letters*, 36, 835
- Johnstone, R. M., Fabian, A. C., & Nulsen, P. E. J. 1987, *MNRAS*, 224, 75
- Jones, C., Forman, W., Vikhlinin, A., Markevitch, M., David, L., Warmflash, A., Murray, S., & Nulsen, P. E. J. 2002, *ApJ*, 567, L115
- Jones, T. W., Porter, D. H., Ryu, D., & Cho, J. 2011, *ArXiv e-prints*
- Jura, M. 1986, *ApJ*, 306, 483
- Kaastra, J. S., Tamura, T., Peterson, J. R., Bleeker, J. A. M., Ferrigno, C., Kahn, S. M., Paerels, F. B. S., Piffaretti, R., Branduardi-Raymont, G., & Böhringer, H. 2004, *A&A*, 413, 415
- Kaiser, N. 1991, *ApJ*, 383, 104
- Kauffmann, G., White, S. D. M., & Guiderdoni, B. 1993, *MNRAS*, 264, 201
- Kim, J.-h., Wise, J. H., Alvarez, M. A., & Abel, T. 2011, *ApJ*, 738, 54
- Kim, W.-T., El-Zant, A. A., & Kamionkowski, M. 2005, *ApJ*, 632, 157
- King, A. R. & Pringle, J. E. 2006, *MNRAS*, 373, L90
- . 2007, *MNRAS*, 377, L25
- King, A. R., Pringle, J. E., & Hofmann, J. A. 2008, *MNRAS*, 385, 1621
- Kirkpatrick, C. C., Gitti, M., Cavagnolo, K. W., McNamara, B. R., David, L. P., Nulsen, P. E. J., & Wise, M. W. 2009, *ApJ*, 707, L69
- Kirkpatrick, C. C., McNamara, B. R., & Cavagnolo, K. W. 2011, *ApJ*, 731, L23+
- Komatsu, E., Smith, K. M., Dunkley, J., Bennett, C. L., Gold, B., Hinshaw, G., Jarosik, N., Larson, D., Nolta, M. R., Page, L., Spergel, D. N., Halpern, M., Hill, R. S., Kogut, A., Limon, M., Meyer, S. S., Odegard, N., Tucker, G. S., Weiland, J. L., Wollack, E., & Wright, E. L. 2011, *ApJS*, 192, 18

- Körding, E., Rupen, M., Knigge, C., Fender, R., Dhawan, V., Templeton, M., & Muxlow, T. 2008, *Science*, 320, 1318
- Kraft, R. P., Vázquez, S. E., Forman, W. R., Jones, C., Murray, S. S., Hardcastle, M. J., Worrall, D. M., & Churazov, E. 2003, *ApJ*, 592, 129
- Krolik, J. H. & Hawley, J. F. 2010, in *Lecture Notes in Physics*, Berlin Springer Verlag, Vol. 794, *Lecture Notes in Physics*, Berlin Springer Verlag, ed. T. Belloni, 265–+
- Krolik, J. H., Hawley, J. F., & Hirose, S. 2005, *ApJ*, 622, 1008
- Kunz, M. W., Schekochihin, A. A., Cowley, S. C., Binney, J. J., & Sanders, J. S. 2011, *MNRAS*, 410, 2446
- Lehnert, M. D., Tasse, C., Nesvadba, N. P. H., Best, P. N., & van Driel, W. 2011, *A&A*, 532, L3
- Lynden-Bell, D. 1969, *Nature*, 223, 690
- Ma, C. ., McNamara, B. R., Nulsen, P. E. J., Schaffer, R., & Vikhlinin, A. 2011, *ArXiv e-prints*
- Machacek, M., Nulsen, P. E. J., Jones, C., & Forman, W. R. 2006, *ApJ*, 648, 947
- Mantz, A., Allen, S. W., Rapetti, D., & Ebeling, H. 2010, *MNRAS*, 406, 1759
- Martin, C. L. 2005, *ApJ*, 621, 227
- Martínez-Sansigre, A. & Rawlings, S. 2011, *MNRAS*, 414, 1937
- Martini, P., Kelson, D. D., Mulchaey, J. S., & Trager, S. C. 2002, *ApJ*, 576, L109
- Martini, P., Sivakoff, G. R., & Mulchaey, J. S. 2009, *ApJ*, 701, 66
- Mathews, W. G. & Brighenti, F. 2003, *ARA&A*, 41, 191
- . 2008, *ApJ*, 685, 128
- Mathews, W. G. & Guo, F. 2010, *ApJ*, 725, 1440
- McCarthy, I. G., Babul, A., Bower, R. G., & Balogh, M. L. 2008, *MNRAS*, 386, 1309
- McCarthy, I. G., Schaye, J., Ponman, T. J., Bower, R. G., Booth, C. M., Dalla Vecchia, C., Crain, R. A., Springel, V., Theuns, T., & Wiersma, R. P. C. 2010, *MNRAS*, 406, 822

- McConnell, N. J., Ma, C.-P., Gebhardt, K., Wright, S. A., Murphy, J. D., Lauer, T. R., Graham, J. R., & Richstone, D. O. 2011, *Nature*, 480, 215
- McDonald, M. 2011, *ApJ*, 742, L35
- McDonald, M., Veilleux, S., Rupke, D. S. N., & Mushotzky, R. 2010, *ApJ*, 721, 1262
- McKinney, J. C., Tchekhovskoy, A., & Blandford, R. D. 2012, *ArXiv e-prints*
- McNamara, B. R., Kazemzadeh, F., Rafferty, D. A., Birzan, L., Nulsen, P. E. J., Kirkpatrick, C. C., & Wise, M. W. 2009, *ApJ*, 698, 594
- McNamara, B. R. & Nulsen, P. E. J. 2007, *ARA&A*, 45, 117
- McNamara, B. R., Nulsen, P. E. J., Wise, M. W., Rafferty, D. A., Carilli, C., Sarazin, C. L., & Blanton, E. L. 2005, *Nature*, 433, 45
- McNamara, B. R. & O’Connell, R. W. 1989, *AJ*, 98, 2018
- McNamara, B. R., Rohanizadegan, M., & Nulsen, P. E. J. 2011, *ApJ*, 727, 39
- McNamara, B. R., Wise, M., Nulsen, P. E. J., David, L. P., Sarazin, C. L., Bautz, M., Markevitch, M., Vikhlinin, A., Forman, W. R., Jones, C., & Harris, D. E. 2000, *ApJ*, 534, L135
- Meier, D. L. 1999, *ApJ*, 522, 753
- Mendygral, P. J., O’Neill, S. M., & Jones, T. W. 2011, *ApJ*, 730, 100
- Merloni, A. & Heinz, S. 2007, *MNRAS*, 381, 589
- Merloni, A., Heinz, S., & Di Matteo, T. 2005, *Ap&SS*, 300, 45
- Miller, J. M. 2007, *ARA&A*, 45, 441
- Miller, L. 1986a, *MNRAS*, 220, 713
- . 1986b, *MNRAS*, 220, 713
- Mittal, R., Hudson, D. S., Reiprich, T. H., & Clarke, T. 2009, *A&A*, 501, 835
- Moderski, R. & Sikora, M. 1996, *MNRAS*, 283, 854
- Morganti, R., Holt, J., Saripalli, L., Oosterloo, T. A., & Tadhunter, C. N. 2007, *A&A*, 476, 735

- Morsony, B. J., Heinz, S., Brüggem, M., & Ruszkowski, M. 2010, *MNRAS*, 407, 1277
- Mulchaey, J. S. & Jeltama, T. E. 2010, *ApJ*, 715, L1
- Nakamura, M., Tregillis, I. L., Li, H., & Li, S. 2008, *ApJ*, 686, 843
- Narayan, R. & Fabian, A. C. 2011, *MNRAS*, 415, 3721
- Narayan, R. & McClintock, J. E. 2008, *New A Rev.*, 51, 733
- . 2012, *MNRAS*, 419, L69
- Narayan, R. & Medvedev, M. V. 2001, *ApJ*, 562, L129
- Narayan, R. & Yi, I. 1994, *ApJ*, 428, L13
- Nemmen, R. S., Bower, R. G., Babul, A., & Storchi-Bergmann, T. 2007, *MNRAS*, 377, 1652
- Nesvadba, N. P. H., Lehnert, M. D., Eisenhauer, F., Gilbert, A., Tecza, M., & Abuter, R. 2006, *ApJ*, 650, 693
- Nipoti, C. & Binney, J. 2005, *MNRAS*, 361, 428
- Noeske, K. G., Weiner, B. J., Faber, S. M., Papovich, C., Koo, D. C., Somerville, R. S., Bundy, K., Conselice, C. J., Newman, J. A., Schiminovich, D., Le Floch, E., Coil, A. L., Rieke, G. H., Lotz, J. M., Primack, J. R., Barmby, P., Cooper, M. C., Davis, M., Ellis, R. S., Fazio, G. G., Guhathakurta, P., Huang, J., Kassin, S. A., Martin, D. C., Phillips, A. C., Rich, R. M., Small, T. A., Willmer, C. N. A., & Wilson, G. 2007, *ApJ*, 660, L43
- Nulsen, P., Jones, C., Forman, W., Churazov, E., McNamara, B., David, L., & Murray, S. 2009, in *American Institute of Physics Conference Series*, Vol. 1201, American Institute of Physics Conference Series, ed. S. Heinz & E. Wilcots, 198–201
- Nulsen, P. E. J., Jones, C., Forman, W. R., David, L. P., McNamara, B. R., Rafferty, D. A., Bîrzan, L., & Wise, M. W. 2007, in *Heating versus Cooling in Galaxies and Clusters of Galaxies*, ed. H. Böhringer, G. W. Pratt, A. Finoguenov, & P. Schuecker, 210
- Nulsen, P. E. J., McNamara, B. R., Wise, M. W., & David, L. P. 2005, *ApJ*, 628, 629
- O’Dea, C. P., Baum, S. A., Privon, G., Noel-Storr, J., Quillen, A. C., Zufelt, N., Park, J., Edge, A., Russell, H., Fabian, A. C., Donahue, M., Sarazin, C. L., McNamara, B., Bregman, J. N., & Egami, E. 2008, *ApJ*, 681, 1035

- Ogle, P., Bou langer, F., Guillard, P., Evans, D. A., Antonucci, R., Appleton, P. N., Nesvadba, N., & Leipski, C. 2010, *ApJ*, 724, 1193
- O’Neill, S. M., De Young, D. S., & Jones, T. W. 2009, *ApJ*, 694, 1317
- O’Neill, S. M. & Jones, T. W. 2010, *ApJ*, 710, 180
- O’Sullivan, E., Giacintucci, S., David, L. P., Gitti, M., Vrtilik, J. M., Raychaudhury, S., & Ponman, T. J. 2011a, *ApJ*, 735, 11
- O’Sullivan, E., Giacintucci, S., David, L. P., Vrtilik, J. M., & Raychaudhury, S. 2011b, *MNRAS*, 411, 1833
- Parrish, I. J., Quataert, E., & Sharma, P. 2009, *ApJ*, 703, 96
- . 2010, *ApJ*, 712, L194
- Parrish, I. J. & Stone, J. M. 2005, *ApJ*, 633, 334
- Parrish, I. J., Stone, J. M., & Lemaster, N. 2008, *ApJ*, 688, 905
- Pedlar, A., Ghataure, H. S., Davies, R. D., Harrison, B. A., Perley, R., Crane, P. C., & Unger, S. W. 1990, *MNRAS*, 246, 477
- Perley, R. A., Dreher, J. W., & Cowan, J. J. 1984, *ApJ*, 285, L35
- Perlmutter, S., Aldering, G., Goldhaber, G., Knop, R. A., Nugent, P., Castro, P. G., Deustua, S., Fabbro, S., Goobar, A., Groom, D. E., Hook, I. M., Kim, A. G., Kim, M. Y., Lee, J. C., Nunes, N. J., Pain, R., Pennypacker, C. R., Quimby, R., Lidman, C., Ellis, R. S., Irwin, M., McMahon, R. G., Ruiz-Lapuente, P., Walton, N., Schaefer, B., Boyle, B. J., Filippenko, A. V., Matheson, T., Fruchter, A. S., Panagia, N., Newberg, H. J. M., Couch, W. J., & The Supernova Cosmology Project. 1999, *ApJ*, 517, 565
- Peterson, J. R. & Fabian, A. C. 2006, *Phys. Rep.*, 427, 1
- Peterson, J. R., Kahn, S. M., Paerels, F. B. S., Kaastra, J. S., Tamura, T., Bleeker, J. A. M., Ferrigno, C., & Jernigan, J. G. 2003, *ApJ*, 590, 207
- Pfrommer, C., Chang, P., & Broderick, A. E. 2011, *ArXiv e-prints*
- Pfrommer, C., Enßlin, T. A., & Sarazin, C. L. 2005, *A&A*, 430, 799
- Pizzolato, F. & Soker, N. 2006, *MNRAS*, 371, 1835
- . 2010, *MNRAS*, 408, 961

- Pratt, G. W., Arnaud, M., Piffaretti, R., Böhringer, H., Ponman, T. J., Croston, J. H., Voit, G. M., Borgani, S., & Bower, R. G. 2010, *A&A*, 511, A85+
- Proga, D. & Begelman, M. C. 2003, *ApJ*, 592, 767
- Punsly, B. 2011, *ApJ*, 728, L17+
- Quataert, E. 2008, *ApJ*, 673, 758
- Rafferty, D. A., McNamara, B. R., & Nulsen, P. E. J. 2008, *ApJ*, 687, 899
- Rafferty, D. A., McNamara, B. R., Nulsen, P. E. J., & Wise, M. W. 2006, *ApJ*, 652, 216
- Randall, S. W., Forman, W. R., Giacintucci, S., Nulsen, P. E. J., Sun, M., Jones, C., Churazov, E., David, L. P., Kraft, R., Donahue, M., Blanton, E. L., Simionescu, A., & Werner, N. 2011, *ApJ*, 726, 86
- Rasera, Y., Lynch, B., Srivastava, K., & Chandran, B. 2008, *ApJ*, 689, 825
- Rebusco, P., Churazov, E., Böhringer, H., & Forman, W. 2005, *MNRAS*, 359, 1041
- Reynolds, C. S., McKernan, B., Fabian, A. C., Stone, J. M., & Vernaleo, J. C. 2005, *MNRAS*, 357, 242
- Riess, A. G., Filippenko, A. V., Liu, M. C., Challis, P., Clocchiatti, A., Diercks, A., Garnavich, P. M., Hogan, C. J., Jha, S., Kirshner, R. P., Leibundgut, B., Phillips, M. M., Reiss, D., Schmidt, B. P., Schommer, R. A., Smith, R. C., Spyromilio, J., Stubbs, C., Suntzeff, N. B., Tonry, J., Woudt, P., Brunner, R. J., Dey, A., Gal, R., Graham, J., Larkin, J., Odewahn, S. C., & Oppenheimer, B. 2000, *ApJ*, 536, 62
- Rizza, E., Loken, C., Bliton, M., Roettiger, K., Burns, J. O., & Owen, F. N. 2000, *AJ*, 119, 21
- Roediger, E., Brüggén, M., Rebusco, P., Böhringer, H., & Churazov, E. 2007, *MNRAS*, 375, 15
- Rosner, R. & Tucker, W. H. 1989, *ApJ*, 338, 761
- Rupke, D. S. N. & Veilleux, S. 2011, *ApJ*, 729, L27
- Russell, H. R., Fabian, A. C., Sanders, J. S., Johnstone, R. M., Blundell, K. M., Brandt, W. N., & Crawford, C. S. 2010, *MNRAS*, 402, 1561
- Ruszkowski, M., Brüggén, M., & Begelman, M. C. 2004, *ApJ*, 611, 158

- Ruszkowski, M., Enßlin, T. A., Brügger, M., Heinz, S., & Pfrommer, C. 2007, MNRAS, 378, 662
- Ruszkowski, M. & Oh, S. P. 2011, MNRAS, 414, 1493
- Salomé, P. & Combes, F. 2003, A&A, 412, 657
- . 2008, A&A, 489, 101
- Salomé, P., Combes, F., Revaz, Y., Downes, D., Edge, A. C., & Fabian, A. C. 2011, A&A, 531, A85
- Sambruna, R. M., Chartas, G., Eracleous, M., Mushotzky, R. F., & Nousek, J. A. 2000, ApJ, 532, L91
- Samuele, R., McNamara, B. R., Vikhlinin, A., & Mullis, C. R. 2011, ApJ, 731, 31
- Sanders, J. S. & Fabian, A. C. 2008, MNRAS, 390, L93
- Sanders, J. S., Fabian, A. C., Frank, K. A., Peterson, J. R., & Russell, H. R. 2010, MNRAS, 402, 127
- Sanders, J. S., Fabian, A. C., & Smith, R. K. 2011, MNRAS, 410, 1797
- Sanders, J. S., Fabian, A. C., & Taylor, G. B. 2009, MNRAS, 396, 1449
- Santos, J. S., Tozzi, P., Rosati, P., & Böhringer, H. 2010, A&A, 521, A64+
- Sarazin, C. L., Burns, J. O., Roettiger, K., & McNamara, B. R. 1995, ApJ, 447, 559
- Sarazin, C. L. & O’Connell, R. W. 1983, ApJ, 268, 552
- Scannapieco, E. & Brügger, M. 2008, ApJ, 686, 927
- Schawinski, K., Thomas, D., Sarzi, M., Maraston, C., Kaviraj, S., Joo, S.-J., Yi, S. K., & Silk, J. 2007, MNRAS, 382, 1415
- Schekochihin, A. A., Cowley, S. C., Kulsrud, R. M., Hammett, G. W., & Sharma, P. 2005, ApJ, 629, 139
- Schekochihin, A. A., Cowley, S. C., Rincon, F., & Rosin, M. S. 2010, MNRAS, 405, 291
- Scheuer, P. A. G. 1974, MNRAS, 166, 513
- Schindler, S., Castillo-Morales, A., De Filippis, E., Schwobe, A., & Wambsganss, J. 2001, A&A, 376, L27

- Shakura, N. I. & Sunyaev, R. A. 1973, *A&A*, 24, 337
- Sharma, P., Chandran, B. D. G., Quataert, E., & Parrish, I. J. 2009, *ApJ*, 699, 348
- Sharma, P., McCourt, M., Quataert, E., & Parrish, I. J. 2011, *astro-ph/1106.4816*
- Siemiginowska, A., Burke, D. J., Aldcroft, T. L., Worrall, D. M., Allen, S., Bechtold, J., Clarke, T., & Cheung, C. C. 2010, *ApJ*, 722, 102
- Sijacki, D., Pfrommer, C., Springel, V., & Enßlin, T. A. 2008, *MNRAS*, 387, 1403
- Sijacki, D. & Springel, V. 2006, *MNRAS*, 366, 397
- Sikora, M., Stawarz, L., & Lasota, J.-P. 2007, *ApJ*, 658, 815
- Silk, J. & Rees, M. J. 1998, *A&A*, 331, L1
- Simionescu, A., Werner, N., Böhringer, H., Kaastra, J. S., Finoguenov, A., Brüggén, M., & Nulsen, P. E. J. 2009, *A&A*, 493, 409
- Simionescu, A., Werner, N., Finoguenov, A., Böhringer, H., & Brüggén, M. 2008, *A&A*, 482, 97
- Smith, D. A., Wilson, A. S., Arnaud, K. A., Terashima, Y., & Young, A. J. 2002, *ApJ*, 565, 195
- Smith, R. K., Brickhouse, N. S., Liedahl, D. A., & Raymond, J. C. 2001, *ApJ*, 556, L91
- Soker, N. 2008, *ApJ*, 684, L5
- Soker, N., White, III, R. E., David, L. P., & McNamara, B. R. 2001, *ApJ*, 549, 832
- Somerville, R. S. & Primack, J. R. 1999, *MNRAS*, 310, 1087
- Sparks, W. B., Macchetto, F., & Golombek, D. 1989, *ApJ*, 345, 153
- Spergel, D. N., Bean, R., Doré, O., Nolta, M. R., Bennett, C. L., Dunkley, J., Hinshaw, G., Jarosik, N., Komatsu, E., Page, L., Peiris, H. V., Verde, L., Halpern, M., Hill, R. S., Kogut, A., Limon, M., Meyer, S. S., Odegard, N., Tucker, G. S., Weiland, J. L., Wollack, E., & Wright, E. L. 2007, *ApJS*, 170, 377
- Springel, V. & Hernquist, L. 2003, *MNRAS*, 339, 289
- Sun, M., Voit, G. M., Donahue, M., Jones, C., Forman, W., & Vikhlinin, A. 2009, *ApJ*, 693, 1142

- Tabor, G. & Binney, J. 1993, MNRAS, 263, 323
- Tacconi, L. J., Genzel, R., Neri, R., Cox, P., Cooper, M. C., Shapiro, K., Bolatto, A., Bouché, N., Bournaud, F., Burkert, A., Combes, F., Comerford, J., Davis, M., Schreiber, N. M. F., Garcia-Burillo, S., Gracia-Carpio, J., Lutz, D., Naab, T., Omont, A., Shapley, A., Sternberg, A., & Weiner, B. 2010, Nature, 463, 781
- Tanaka, Y., Nandra, K., Fabian, A. C., Inoue, H., Otani, C., Dotani, T., Hayashida, K., Iwasawa, K., Kii, T., Kunieda, H., Makino, F., & Matsuoka, M. 1995, Nature, 375, 659
- Tchekhovskoy, A., Narayan, R., & McKinney, J. C. 2010, ApJ, 711, 50
- . 2011, astro-ph/1108.0412
- Tucker, W. & David, L. P. 1997, ApJ, 484, 602
- Urry, C. M. & Padovani, P. 1995, PASP, 107, 803
- Veilleux, S., Cecil, G., & Bland-Hawthorn, J. 2005, ARA&A, 43, 769
- Vernaleo, J. C. & Reynolds, C. S. 2007, ApJ, 671, 171
- Vikhlinin, A., Burenin, R., Forman, W. R., Jones, C., Hornstrup, A., Murray, S. S., & Quintana, H. 2007, in Heating versus Cooling in Galaxies and Clusters of Galaxies, ed. H. Böhringer, G. W. Pratt, A. Finoguenov, & P. Schuecker , 48–+
- Vikhlinin, A., Kravtsov, A. V., Burenin, R. A., Ebeling, H., Forman, W. R., Hornstrup, A., Jones, C., Murray, S. S., Nagai, D., Quintana, H., & Voevodkin, A. 2009, ApJ, 692, 1060
- Vikhlinin, A., Markevitch, M., Murray, S. S., Jones, C., Forman, W., & Van Speybroeck, L. 2005, ApJ, 628, 655
- Voigt, L. M. & Fabian, A. C. 2004, MNRAS, 347, 1130
- Voit, G. M. 2005, Reviews of Modern Physics, 77, 207
- . 2011, astro-ph/1107.2142
- Voit, G. M., Cavagnolo, K. W., Donahue, M., Rafferty, D. A., McNamara, B. R., & Nulsen, P. E. J. 2008, ApJ, 681, L5
- Voit, G. M. & Donahue, M. 2005, ApJ, 634, 955

- . 2011, *ApJ*, 738, L24+
- Volonteri, M., Madau, P., Quataert, E., & Rees, M. J. 2005, *ApJ*, 620, 69
- Volonteri, M. & Stark, D. P. 2011, *MNRAS*, 1331
- Werner, N., Simionescu, A., Million, E. T., Allen, S. W., Nulsen, P. E. J., von der Linden, A., Hansen, S. M., Böhringer, H., Churazov, E., Fabian, A. C., Forman, W. R., Jones, C., Sanders, J. S., & Taylor, G. B. 2010, *MNRAS*, 407, 2063
- Willott, C. J., Rawlings, S., Blundell, K. M., & Lacy, M. 1999, *MNRAS*, 309, 1017
- Wilman, R. J., Edge, A. C., & Swinbank, A. M. 2009, *MNRAS*, 395, 1355
- Wilson, A. S. & Colbert, E. J. M. 1995, *ApJ*, 438, 62
- Wong, K.-W., Irwin, J. A., Yukita, M., Million, E. T., Mathews, W. G., & Bregman, J. N. 2011, *ApJ*, 736, L23+
- Worrall, D. M. 2009, *A&A Rev.*, 17, 1
- Wu, K. K. S., Fabian, A. C., & Nulsen, P. E. J. 2000, *MNRAS*, 318, 889
- Wu, Q., Cao, X., & Wang, D.-X. 2011, *ApJ*, 735, 50
- Young, O. E., Thomas, P. A., Short, C. J., & Pearce, F. 2011, *MNRAS*, 413, 691
- Zakamska, N. L. & Narayan, R. 2003, *ApJ*, 582, 162
- ZuHone, J. A., Markevitch, M., & Johnson, R. E. 2010, *ApJ*, 717, 908